UNCLASSIFIED CONFIDENTIAL

Copy 6
RM E56G24
c.2

NACA RM E56G24

NACA

RESEARCH MEMORANDUM

EXPERIMENTAL INVESTIGATION OF A FIVE-STAGE AXIAL-FLOW RESEARCH COMPRESSOR WITH TRANSONIC ROTORS IN ALL STAGES

III - INTERSTAGE DATA AND INDIVIDUAL STAGE PERFORMANCE CHARACTERISTICS

By Donald M. Sandercock and Karl Kovach

Lewis Flight Propulsion Laboratory
Cleveland, Ohio

NATIONAL ADVISORY COMMITTEE
FOR AERONAUTICS

WASHINGTON

October 10, 1956

CONFIDENTIAL
UNCLASSIFIED

NACA RM E56G24

NATIONAL ADVISORY COMMITTEE FOR AERONAUTICS

RESEARCH MEMORANDUM

EXPERIMENTAL INVESTIGATION OF A FIVE-STAGE AXIAL-FLOW RESEARCH COMPRESSOR WITH TRANSONIC ROTORS IN ALL STAGES

III - INTERSTAGE DATA AND INDIVIDUAL STAGE PERFORMANCE CHARACTERISTICS

By Donald M. Sandercock and Karl Kovach

SUMMARY

In order to study the detailed performance of the individual blade rows of a five-stage axial-flow compressor, radial distributions of total pressure, total temperature, static pressure and air-flow angle were obtained at the exit of each blade row. These data are tabulated for a range of flows at equivalent tip speeds of from 70 to 100 percent of design. Individual stage performance curves in terms of flow coefficient, equivalent total-pressure ratio, equivalent temperature-rise ratio, and adiabatic efficiency are presented and evaluated.

An overcambering of the inlet stages plus an excessive annulus area from the first-stage exit to the compressor-discharge station caused the stages to be mismatched at design speed but favorably affected the low-speed performance, the best compressor match point occurring between 80 and 90 percent of equivalent design speed.

INTRODUCTION

Numerous examples of the potentials of axial-flow-compressor stages operating with rotor tip relative Mach numbers in the transonic range to produce high pressure ratio and high specific weight flow have been reported, a few of which are listed in references 1 to 4. To study the problems associated with the combining of these high-performance stages, a five-stage 20-inch-diameter compressor was designed and constructed at the NACA Lewis laboratory. The design details of this compressor are discussed in reference 5, and the over-all performance is presented in reference 6.

The over-all performance (ref. 6) indicates that at design total-pressure ratio and design speed a higher than design corrected weight flow was obtained at a lower than over-all design value of adiabatic efficiency. Peak compressor efficiency occurred at a lower than design speed, indicating that the stages were more closely matched at some off-design speed. Reference 6 speculates on the effects of the higher than design equivalent weight flow, design boundary-layer allowances, and an overcambering of some blade rows, which may have resulted in some mismatching of the stages at design speed.

To study the performance of the individual stages, three series of tests were run, during which groups of blade rows were instrumented successively. Each series of test points covered a range of air flow from choke to the approximate compressor surge limit or limiting turbine-inlet 4154
temperature for speeds from 70 to 100 percent of equivalent design speed. During each test run radial distributions of total pressure, static pressure, total temperature, and air angle were obtained.

This report presents these radial distributions of performance data in tables and in curves of average individual stage performance characteristics in terms of flow coefficient, stage equivalent pressure ratio, stage equivalent temperature-rise ratio, and stage adiabatic efficiency over the range investigated.

SYMBOLS

A annulus area, sq ft

M Mach number

N rotational speed, rpm

P total or stagnation pressure, lb/sq ft

p static or stream pressure, lb/sq ft

r radius, in.

s blade spacing, in.

ds differential distance measured along the circumferential direction covered by the wake rake

T total or stagnation temperature, $^{\circ}R$

U rotor speed, ft/sec

V_{fl} volume flow, cu ft/sec

w weight-flow rate, lb/sec

β air angle, angle between air velocity and axial direction, deg

δ ratio of total pressure to NACA standard sea-level pressure of 2116 lb/sq ft

η temperature-rise efficiency

η_M momentum efficiency

θ ratio of total temperature to NACA standard sea-level temperature of 518.7° R

φ flow coefficient

4154

Subscripts:

C combination probe

e equivalent, indicates that parameter to which it is affixed has been corrected to that which would be obtained at design speed

CQ-1 back

h hub

n station number (see fig. 2)

t tip

WR wake rake

0 bellmouth inlet (fig. 2)

1 compressor flow-measuring station (fig. 2)

2 compressor first-rotor inlet

3,5,7,9,11 interstage measuring stations at exit of first, second, . . . fifth rotors (fig. 2)

4,6,8,10,12 interstage measuring stations at exit of first, second, . . . fifth stators (fig. 2)

APPARATUS AND INSTRUMENTATION

Compressor Installation

A description of the aerodynamic design and geometry of the compressor used for this investigation is presented in reference 5, and the over-all performance is given in reference 6. The stage performance data reported herein were obtained with the compressor operating as a component of a turbojet engine. The installation of the compressor in the engine is described in reference 6. Figure 1 is a photograph of the engine installation.

Instrumentation

Engine bellmouth inlet. - The instrumentation at the engine bell- 4154
mouth inlet (station 0, fig. 2) was the same as that reported in reference 6.

Compressor flow-measuring station. - The location and instrumentation used at the compressor flow-measuring station (station 1, fig. 2) was the same as reported in reference 6, with the following exception. In place of the boundary-layer rakes, two radial total-temperature rakes were installed. The rakes were 180° apart, and each contained five shielded thermocouples equally spaced across the passage.

Compressor inlet. - The location of wall static-pressure taps at the compressor inlet (station 2, fig. 2) is described in reference 6. In addition, in the same axial plane an actuator-mounted, self-balancing, wedge-type static-pressure probe (fig. 3(c)) was used to survey the passage.

Survey stations. - Radial surveys were made at stations 3 to 12 inclusive (fig. 2) using combinations of the following instruments:

(1) A combination probe (fig. 3(a)), which consists of a single total pressure, an angle-sensing claw, and two slotted-shield stagnation thermocouples. The probe was actuator-mounted and self-balancing. The thermocouples were calibrated for Mach number and density effects.

(2) A sting-mounted, wedge-type static-pressure probe (fig. 3(b)) with separate static-pressure orifices located on both sides of the wedge. This probe was mounted in an actuator and made self-balancing. Calibration tests of this probe provided a Mach number correction and showed that radial flows of the magnitude anticipated from this compressor hub configuration and free-vortex type of velocity diagram used in the design had a negligible effect on the probe readings.

(3) A wake rake (fig. 3(d)), which consisted of 19 total-pressure tubes mounted circumferentially. Fourteen of the tubes were spaced 0.060 inch apart to define the blade wake, and the end tubes were spaced farther apart to record the free-stream pressure. The rake covered at least one blade spacing at all radial positions.

Behind each rotor row two combination probes and a single static-pressure probe were used. At each stator exit a wake rake and a static-pressure probe were employed. In addition, behind the stator rows of the first and second stages, three combination probes were spaced so that one instrument traversed radially the center of a blade passage and the remaining two instruments traversed the portions of the blade passage adjoining the suction and pressure surfaces of the blades. Behind the third, fourth, and fifth stages, only the combination probes covering the center portion and the portion of the passage close to the pressure surface of the blade were used. In each case an attempt was made to keep the combination probes out of the blade wakes. The approximate circumferential location of the probes for each of the series of tests is presented in figure 4. In order to minimize the blockage effect of the large number of instruments, all probes were designed with small frontal area over the portion of the stem extending into the airstream.

Four static-pressure orifices, equally spaced circumferentially, were located at the outer wall at each measuring station. The axial distance from the measuring station to the blade trailing edge varied from 0.40 inch at the hub to from 0.60 to 0.80 inch at the tip behind the rotor blades and was approximately constant at 0.25 inch behind the stator blade rows.

Pressures were measured with manometers containing either mercury or tetrabromoethane. Temperatures and angles were measured and recorded with a self-balancing digital potentiometer that recorded readings at the rate of approximately two per second. Compressor speed was measured with a chronometric tachometer.

PROCEDURE

Operation

All tests were conducted with ambient-air inlet conditions; consequently, no control of the compressor-inlet conditions could be employed. Since instrumenting all blade rows simultaneously would have required a prohibitively large number of actuators, three series of tests were run during which several blade rows were instrumented successively. The first series provided data from the first and second stages; the second series, from the third and fourth stages; and the third series, from the fifth stage. For each series the compressor was operated at constant equivalent speeds of 70, 80, 90, and 100 percent of design. The range of air flow covered at each speed was achieved by means of an adjustable exhaust nozzle such as was used for the over-all performance tests described in reference 6. For these tests, however, only the first-stage turbine stators that gave maximum pressure ratio at design speed were used.

Typical Test Run

A typical test point was run in the following manner: With all instruments pulled out to the outer-wall position (radial position 1, table I), the compressor equivalent speed was set and a stable operating condition noted. While the instruments behind the stator rows remained at the outer wall, data were recorded from all the instruments behind the rotor rows at 11 radial positions (radial positions 2 to 12, table I). The rotor-exit survey instruments were then retracted to the outer wall and remained there while the passage was surveyed with the instruments 4154
behind the stator rows. During the complete test run, a constant check on the compressor-inlet temperature and compressor speed was maintained in order that the equivalent compressor speed could be held essentially constant. At each radial position total and static pressures were recorded once on film while each angle was recorded three times and each temperature twice on a digital potentiometer. This procedure yielded a time as well as circumferential variation of the data. The compressor-inlet temperature (an average of 10 thermocouples, station 1) was recorded at each radial survey position. The running time necessary to complete a test run was approximately $1\frac{1}{2}$ hours.

Calculation

Data necessary to compute conditions at the inlet to the first rotor (series 1) were obtained by assuming a radially constant value of total temperature and total pressure equal to the measured compressor-inlet total temperature (station 1) and the barometer reading minus 0.10 inch of mercury, respectively. The drop of 0.10 inch of mercury from the barometer pressure was used to account for the pressure drop across the four struts in the inlet section and any other flow losses in the bellmouth. The radial distribution of static pressure was obtained from a series of static-pressure surveys at station 2 covering the compressor speed and weight-flow range. The results of these surveys are plotted as a function of corrected compressor weight flow in figure 5. The inlet surveys served to validate the assumption that the air entering the first rotor had no prewhirl. For series 2 and 3 the necessary data to compute the inlet conditions to the third and fifth stages, respectively, were obtained from a survey with a single combination probe. These data were correlated with the stator-outlet data of the preceding series and a static-pressure distribution obtained by correcting the static pressures measured at a previous series run by the ratio of the average values of the wall static taps.

Because of the choke and surge limits of the compressor, a complete flow range of any given stage cannot be realized for a given speed. However, within certain limitations, the stage performance may be presented as average values of flow coefficient φ, equivalent pressure ratio $(P_n/P_{n-2})_e$, equivalent temperature-rise ratio $\left[\frac{\Delta T_{n-(n-2)}}{T_{n-2}}\right]_e$, and adiabatic efficiency η, which results in a single performance curve that is essentially independent of speed as long as compressibility effects are small. This curve represents the approximate curve that would be obtained if the complete flow range of the given stage could be covered at design speed.

A complete derivation of these dimensionless performance parameters is given in reference 7, and their use and limitations when employed in conjunction with transonic and high-performance stages are illustrated in reference 8. In the investigation reported herein, blade tip speed and mass-averaged values of stage pressure ratio and temperature-rise ratio were used in place of the mean blade speed and arithmetically averaged values of stage pressure ratio and temperature-rise ratio used in reference 8. Compressor weight flows were computed from data obtained at station 1 (fig. 2) as explained in reference 6.

PRESENTATION OF SURVEY DATA

The data obtained from the survey tests are presented in table II. Since all the results were not gathered under the same compressor-inlet conditions, pressures and temperatures are presented as a ratio to the compressor-inlet (station 2, fig. 2) total pressure and total temperature. Figure 6 presents plots of total pressure and total temperature when the compressor is operating near peak efficiency for speeds of 70, 80, and 90 percent of design speed and at design pressure ratio for design speed. Additional information listed for convenience in table II includes the Mach number associated with the listed values of static and total pressure and the equivalent weight flow, by means of which each run may be associated with the values of figures 5 and 7. Blade geometry necessary to compute certain streamline flow parameters may be obtained from reference 5.

For identification purposes and as an aid in stacking the stages for a given engine operating condition, the series number and engine exhaust-nozzle and bleed settings are listed for each test point in table II. As the exhaust-nozzle setting increases, the nozzle area decreases. This inverse relation between the exhaust-nozzle setting and the area of the exhaust nozzle is only relative, and no absolute values of area were associated with the settings used. The bleeding of air at the compressor discharge was required for acceleration purposes, as described in reference 6.

At each rotor-exit station, the data presented represent the following:

(1) Total pressure is an average from two probes, each recorded once (two values).

(2) Total temperature is an average from four thermocouples, each recorded twice (eight values).

(3) Angle is an average from two probes, each recorded three times 4154
(six values).

(4) Static pressure is a value obtained from a smooth curve faired through the values from a single static probe and intersecting the outer wall at a value from one of four wall static taps. At station 3, where a circumferential variation of several inches of mercury among the wall taps existed, the entire level of static pressure was adjusted until the outer-wall value was equal to the average of the four outer-wall taps. This adjustment was unnecessary at any of the other rotor-exit stations.

At each stator blade-row exit the data presented represent the following:

(1) Total-pressure values are obtained by using the wake rake and combination probe total-pressure values according to the equation

$$P = \frac{\int_{\text{tube 1}}^{\text{tube 19}} P_{WR}\, ds - aP_C}{s}$$

where a is the difference between the circumferential distance covered by the wake rake and 1 blade spacing (consequently, a varies with the radial location); P_C is the average total pressure of the two or three combination probes used; and P_{WR} represents the total-pressure values obtained from tubes on the wake rake.

(2) Total temperature is an average of four or six thermocouples (depending on whether two or three combination probes were used), each recorded twice (either eight or twelve values).

(3) Static pressure is a value obtained from a smooth curve faired through the radial variation of the single probe readings and into the average of four wall static-pressure taps.

(4) Angle is an average from two or three probes (depending on whether two or three combination probes were used), each recorded three times (either six or nine values).

In order to facilitate the use of the recorded data in computing blade element (or streamline) performance parameters, radial survey positions 4 to 10 inclusive at each station were located along the same streamlines according to the definition

$$\frac{r_t - r}{r_t - r_h} = \text{constant}$$

where r is the radius at which the streamline intersects the measuring plane. This is the same definition of a streamline as was used in the design procedure (see ref. 5). The principal discrepancies between the assumed streamline location and the radial probe position arise from the limitations of the prepositioning system used to set the probe radial locations (max. error of 0.025 in.) and at the fourth-stator discharge (station 10) where a compromise was necessary in order that the prepositioning system could be used for the fifth-stage surveys. However, at station 10 for radial positions 8 to 10, where the largest discrepancy exists, the data recorded at all speeds are relatively constant with radius; thus, little error in the calculation of blade-element performance parameters would be anticipated even though radial probe positions rather than assumed streamline locations are used. The additional radial survey positions were used for integrating purposes and to gain some knowledge of boundary-layer thicknesses. All radii for the radial survey positions as well as compressor hub values are presented in table I.

RELIABILITY

The criteria used as an estimate of the accuracy and consistency of the data obtained from this investigation are the ones generally used in an experimental investigation of a compressor stage, namely

(1) A comparison of the integrated weight flow at each survey station with the compressor-inlet weight flow

(2) A comparison of integrated momentum and temperature-rise efficiencies

(3) A comparison of total temperatures at the rotor- and stator-exit stations

However, it is realized that, as the increased number of blade rows provide additional sources for accentuating the unsteadiness and circumferential variation of the airstream, it becomes increasingly more difficult with the type and number of instruments used in these tests to obtain average values of performance data. This was demonstrated in the recording of temperatures and angles, where in many instances the time variation of data from a single probe was as large as or larger than the circumferential variation of the two different probes. Consequently, the standards of these comparisons of weight flow and efficiencies advanced in the more closely controlled single-stage tests will not be applicable to the results presented herein. In addition, the inherent errors in probe settings and calibration, recording of the data, and computational procedure are always present. An attempt was made to keep this latter type of error at a minimum by a careful screening of the data and use of probes.

The weight flows obtained in these series of tests are compared in figure 7. This figure also indicates at the maximum weight-flow points the variation of the compressor-inlet corrected weight flows obtained 4154
with the same engine geometry and equivalent speed for the three series of tests. The integrated momentum and temperature-rise efficiencies are compared in figure 8. The total temperatures at the rotor- and stator-exit stations may be compared in figure 6 or table II.

STAGE PERFORMANCE

The choke and surge limits imposed by the compressor restrict the flow range of a particular stage at any given speed. However, within certain limitations (see ref. 8) performance curves that are approximately those which would be obtained if the complete flow range of the stage could be covered at design speed may be computed by employing equivalent stage performance parameters. These equivalent curves are useful in determining stage matching and in indicating improperly designed stages, and also assist in pointing out regions of operation where the data may be of questionable accuracy.

The flow coefficient ($\varphi = V_{fl}/U_t A$) is defined as the ratio of the volume flow divided by the blade tip speed and a flow area at the entrance to each stage. One approach in selecting a flow area is by use of the concept of dividing the flow into a main or "free-stream" portion where the viscosity effects of the fluid on the flow are negligible and a small or boundary-layer portion near the casing walls where the viscosity effects on the flow are appreciable. The flow coefficient is more representative of the average angle of incidence on each stage if an effective or free-stream flow area is used. However, for simplicity, and because of the difficulty in computing accurate values of effective flow areas from the measured data, the total annulus area was employed in the computations of measured flow coefficients reported herein. The original design values of flow coefficient were obtained from free-stream values of axial velocity. For comparative purposes, therefore, it was necessary to adjust the design values of flow coefficient by means of the assumed design weight-flow blockage factors. Thus, observed differences between design and measured flow coefficients may be due to some extent to differences in the design and measured blockage factors.

No attempt was made to adjust the original design (free-stream) values of total pressure and efficiency for wall boundary-layer effects. It is possible that a more realistic average design value based on the distribution from hub to tip of total annulus area might be somewhat less than the original design (free-stream) values, but it is believed that such differences are insignificant for both total pressure and efficiency.

First Stage

The performance characteristics of the first stage are presented in figure 9(a). Although this stage operates over a narrow range of flow coefficient at each equivalent speed, it operates over a wide range of flow coefficient (or incidence angle) for the range of speeds investigated.

Design flow coefficient was obtained at 90 percent of equivalent design speed, where the performance curves indicate that a higher than design value of energy addition and pressure ratio is attained. Since the design and measured values of efficiency at this flow coefficient are approximately the same, the increased work input could result from a higher than design turning of the air (overcambering of the rotor blades) or the effect of an excessive annulus area at the stage discharge station on the axial velocity ratio across the rotor row. The design values of boundary-layer blockage allowance for the first stage were obtained from the performance results of a single-stage transonic compressor. By elimination, then, the rotor blade overcambering is apparently the cause of the higher than design performance at design flow coefficient (incidence angle). More recent considerations of blade-element data (ref. 9) also indicate that the blade camber, especially in the tip region, was too high. This same result was speculated on in reference 6 on the basis of wall static-pressure measurements.

The higher than design weight flow obtained at design speed forced the first stage to operate at a higher than design flow coefficient (lower than design incidence angle). Consequently, although the design energy addition was attained (overcambering of rotor blades), the poor efficiency resulted in a lower than design pressure ratio.

The location of the 70-percent-speed points on the stall portion of the stage performance curve suggests the use of caution when employing the data obtained at this speed. A hot wire installed behind the first rotor indicated that while a well-defined rotating-stall region could not be observed, the flow at these speeds was of a highly unsteady nature. This region begins at a flow coefficient of 0.47 and extends over the complete flow range (to $\varphi = 0.42$) at 70 percent of design speed.

Second Stage

The second-stage performance characteristics are presented in figure 9(b). The range of flow coefficient over which the second stage operates is slightly smaller than that of the first stage, with all points apparently outside a stage stall region. However, the small margin between the peak and design values of equivalent pressure ratio and temperature-rise ratio is not typical of a stage whose blade sections are designed to operate at their minimum-loss incidence angles. 4154

At design speed a slightly higher than design energy addition was obtained, but the low stage efficiency (indicating high losses at the lower than design incidence angles due to the high flow and low first-stage pressure ratio) resulted in a lower than design pressure ratio. As before, more recent examination of blade-element data indicates an overcambering of the second-rotor blade row also. No evaluation of the possible effects of any discrepancies between the design and actual effective flow areas on the axial velocity ratio can be made for this stage.

Third Stage

The third-stage performance parameters are presented in figure 9(c). The third stage is typical of an intermediate stage of a multistage compressor that operates over a small range of flow coefficient (incidence angle) with considerable overlapping of the individual speed curves.

The third stage did not produce design energy addition at any of the speeds investigated. One reason for the difference between the measured and design energy addition may be that the design camber of the rotor was too low, thus restricting the rotor blades from turning the air through the desired angle. A second possibility is that the design deviation angle of the second-stage stator blades was too low. Insufficient turning in the second-stage stator row would adversely affect both the incidence angle and the inlet Mach number entering the third-stage rotor, thus displacing the third-stage performance curves toward lower values of flow coefficient and energy addition. However, no evaluation of the various possibilities is made at this time.

Fourth Stage

The fourth-stage performance characteristics are presented in figure 9(d). The range of flow coefficient covered is small and shows an overlapping of the individual speed curves, with all operation on the negative-slope side of the curve of equivalent total-pressure ratio.

The higher than design values of pressure ratio and temperature-rise ratio measured across this stage at design speed combine to give an actual value of adiabatic efficiency higher than that assumed in the design of this stage. Although the data in table II (or fig. 6) indicate a difference between the total temperature measured behind the rotor row and that measured behind the stator row, either value shows that this stage produced a higher than design energy addition, though reservations on the quantitative values of the temperature-rise ratio and efficiency are necessary.

Fifth Stage

The performance characteristics of the fifth stage are presented in figure 9(e). Typically, the required range of flow coefficient covered by this exit stage is larger than that covered by the intermediate stages. Also, this stage operates exclusively on the negative slope of the curve of equivalent total-pressure ratio.

At design speed the fifth stage produced a higher than design energy addition and pressure ratio at approximately the assumed design value of adiabatic efficiency. However, because of the multiple factors affecting stage performance, including blade camber, area ratio (or boundary-layer blockage), efficiency, and so forth, no evaluation of the reason for this performance is made at this time.

Stage Matching

The attainment of the compressor design-point performance requires not only that each individual stage reach its design performance but that all stages reach their design points at a specific compressor weight flow. The proper matching of the stages is determined by the flow coefficient, which is a measure of the average, or mean, axial velocity entering each stage. Flow coefficient is affected by the design variation of effective flow area and density ratio, which in turn depends upon the production by each stage of its design pressure ratio of the assumed stage efficiency and the proper boundary-layer blockage.

The point selected for a stage-matching evaluation was the design-speed point at which the compressor produced the design total-pressure ratio. At this operating point the higher than design weight flow forces the first stage to operate at a higher than design flow coefficient on the choked portion of the curves of equivalent total-pressure ratio. At this mode of operation the first stage produced a lower than design total-pressure ratio and work input. The combination of increased flow and below design performance of the first stage should force an increasing difference between the design and the measured flow coefficient entering the second stage if the effective flow area is correct. Figure 9(b) shows that this did occur. This is an additional indication that the design boundary-layer blockage allowance across the first stage was correct.

The second stage is now also forced to operate on the negative portion of the curve of equivalent total-pressure ratio, with the consequent below design performance, although the energy addition was slightly higher than the design value. Continuing this type of reasoning across the third stage, where both the stage temperature rise and pressure ratio are below the design values, it appears that, if the design variation of effective flow area is correct, a large difference should exist between the design and measured values of flow coefficient entering the third and especially the fourth stages.

Actually, figures 9(c), (d), and (e) show that the flow coefficients entering the third, fourth, and fifth stages continuously approach the design values, although the fifth stage had the assistance of the fourth stage, which produced a higher than design density ratio. This could only occur if an excessive annulus area existed from the exit of the first stage to the fifth stage. A further indication of an excessive annulus area extending to the compressor discharge is presented in reference 6. Design-speed values in figure 8 of reference 6 show that at approximately the design pressure ratio and slightly lower than design efficiency, the compressor discharge velocity (axial in direction) was lower than the design value even though a higher than design equivalent weight flow flowed past this area.

Sources for this excessive annulus area include rotor blade overcambering, excessive design boundary-layer blockage allowance, and assumed design rotor efficiencies that were too low. Indications of overcambering of some blade rows have already been noted. From reference 5 the design values of weight-flow blockage factor were assumed for all stages except the first one, and the assumed blade-element efficiencies were believed to be low. From the first-stage exit to the fourth-stage entrance where the measured efficiencies are below or approximately equal to the design values and the stage performances are lower than design, the area allowances for boundary layer are apparently too large and are the main cause for the excessive annulus area. Across the remaining portion of the compressor the relative effects of each of these sources on the axial velocity, or annulus area, could not be separated at this time, although it is believed that the blockage allowance is responsible for the major share of the excess annulus area.

This evidence of overcambering in the inlet stages plus a higher than design axial velocity diffusion throughout the compressor gives further verification to the speculation of reference 6 that this compressor could not have operated at its design weight flow. Operation of these inlet stages closer to their design flow coefficients with the accompanying increase in performance would have forced the latter stages over on the stalled portion of their equivalent performance curves. The best match point of the compressor appears to be attained in the speed range between 80 and 90 percent of design speed, since in this region all the stages are operating on the negative-slope portions of their stage pressure-ratio curves at more favorable angles of attack than those at design speed. This fact is reflected in the increased efficiency of the first two stages as well as in the location of the peak over-all compressor efficiency in this speed range (see ref. 6).

SUMMARY OF RESULTS

The radial distributions of performance data at speeds from 70 to 100 percent of equivalent design speed for a flow range from compressor choke to approximate compressor surge have been tabulated for all stages of a five-stage transonic compressor. From this data plus the blade geometric properties, any desired streamline parameters may be computed.

From an analysis of the individual stage performance, the following conclusions were obtained:

1. The first and second stages showed definite indications of overcambering. However, at design speed the high losses associated with inlet relative Mach numbers in the transonic range and low incidence angles (higher than design flow coefficient) caused both stages to produce a lower than design pressure ratio. The third stage did not produce design energy addition at any point over its entire flow range. The fourth and fifth stages operated closer to the peaks of their pressure-ratio curves, and both produced a higher than design energy addition at design speed. The effects of blade camber, area ratio (or boundary-layer blockage), and efficiency on the stage performance could not be separated and evaluated. For the fourth stage some reservations on the quantitative values of energy addition and efficiency computed at design speed are indicated because of a difference in the temperature recorded behind the fourth rotor and stator rows.

2. At the design-speed and design-pressure-ratio point the combination of overcambering of some blade rows and an excessive annulus area from the first-stage exit to the compressor discharge caused this compressor to seek an equilibrium operating condition at a higher than design weight flow. Under these conditions the inlet stages were forced to operate on the choked portion of their respective stage curves, with an accompanying depreciation of stage performance. However, the latter stages operated closer to their peak stage pressure ratios, thus producing the compressor over-all design total-pressure ratio although at a cost of several points in the assumed over-all efficiency.

3. The overcambering and the excessive values of annulus area, which caused the stages to be mismatched at design speed, probably helped the low-speed performance, the best match point for all stages occurring in the range between 80 and 90 percent of design speed.

Lewis Flight Propulsion Laboratory
National Advisory Committee for Aeronautics
Cleveland, Ohio, July 26, 1956

REFERENCES

1. Lieblein, Seymour, Lewis, George W., Jr., and Sandercock, Donald M.: Experimental Investigation of an Axial-Flow Compressor Inlet Stage Operating at Transonic Relative Inlet Mach Numbers. I - Over-All Performance of Stage with Transonic Rotor and Subsonic Stators up to Rotor Relative Inlet Mach Number of 1.1. NACA RM E52A24, 1952. 4154

2. Serovy, George K., Robbins, William H., and Glaser, Frederick W.: Experimental Investigation of a 0.4 Hub-Tip Diameter Ratio Axial-Flow Compressor Inlet Stage at Transonic Inlet Relative Mach Numbers. I - Rotor Design and Over-All Performance at Tip Speeds from 60 to 100 Percent of Design. NACA RM E53I11, 1953.

3. Robbins, William H., and Glaser, Frederick W.: Investigation of an Axial-Flow-Compressor Rotor with Circular-Arc Blades Operating up to a Rotor-Inlet Relative Mach number of 1.22. NACA RM E53D24, 1953.

4. Wright, Linwood C., and Wilcox, Ward W.: Investigation of Two-Stage Counterrotating Compressor. II - First-Rotor Blade-Element Performance. NACA RM E56G09, 1956.

5. Sandercock, Donald M., Kovach, Karl, and Lieblein, Seymour: Experimental Investigation of a Five-Stage Axial-Flow Research Compressor with Transonic Rotors in All Stages. I - Compressor Design. NACA RM E54F24, 1954.

6. Kovach, Karl, and Sandercock, Donald M.: Experimental Investigation of a Five-Stage Axial-Flow Research Compressor with Transonic Rotors in All Stages. II - Compressor Over-All Performance. NACA RM E54G01, 1954.

7. Medeiros, Arthur A., Benser, William A., and Hatch, James E.: Analysis of Off-Design Performance of a 16-Stage Axial-Flow Compressor with Various Blade Modifications. NACA RM E52L03, 1953.

8. Voit, Charles H., and Geye, Richard P.: Investigation of a High-Pressure-Ratio Eight-Stage Axial-Flow Research Compressor with Two Transonic Inlet Stages. III - Individual Stage Performance Characteristics. NACA RM E54H17, 1954.

9. Robbins, William H., Jackson, Robert J., and Lieblein, Seymour: Blade-Element Flow in Annular Cascades. Ch. VII of Aerodynamic Design of Axial-Flow Compressors, vol. II. NACA RM E56B03a, 1956.

4154

CQ-3

TABLE I. - RADII FOR RADIAL-SURVEY POSITIONS

[Tip radius constant at 10 in.]

Radial position	Radius, r, in., at station -										
	2	3	4	5	6	7	8	9	10	11	12
1		9.900	9.900	9.900	9.900	9.900	9.900	9.900	9.900	9.900	9.900
2		9.850	9.850	9.850	9.850	9.850	9.850	9.850	9.900	9.900	9.900
3		9.650	9.600	9.650	9.700	9.750	9.750	9.750	9.800	9.800	9.800
4	9.167	9.250	9.350	9.450	9.500	9.600	9.600	9.650	9.700	9.700	9.700
5	8.750	8.850	9.000	9.200	9.300	9.400	9.450	9.500	9.550	9.550	9.550
6	8.334	8.500	8.700	8.900	9.050	9.150	9.250	9.350	9.400	9.400	9.400
7	7.501	7.750	8.050	8.400	8.550	8.750	8.850	9.000	9.100	9.100	9.100
8	6.668	6.950	7.400	7.850	8.050	8.350	8.500	8.650	8.850	8.850	8.850
9	6.251	6.600	7.050	7.550	7.850	8.150	8.300	8.500	8.700	8.700	8.700
10	5.835	6.200	6.700	7.300	7.600	7.900	8.100	8.300	8.550	8.550	8.550
11		5.900	6.550	7.150	7.450	7.800	8.000	8.200	8.450	8.450	8.450
12		5.700	6.350	7.000	7.350	7.700	7.900	8.150	8.400	8.400	8.400
Hub		5.456	6.064	6.764	7.102	7.502	7.720	7.976	8.114	8.250	8.250

[redacted]

TABLE II. - RADIAL DISTRIBUTION OF PERFORMANCE DATA FROM FIVE-STAGE TRANSONIC COMPRESSOR

(a) Series 1.

1. Speed, 70-percent design.

Radial position	Station 3					Station 4					Station 5					Station 6				
	P_3/P_2	T_3/T_2	p_3/P_2	β, deg	M	P_4/P_2	T_4/T_2	p_4/P_2	β, deg	M	P_5/P_2	T_5/T_2	p_5/P_2	β, deg	M	P_6/P_2	T_6/T_2	p_6/P_2	β, deg	M
Exhaust-nozzle setting, 0; bleed open; $w\sqrt{\theta}/\delta$, 41.34 lb/sec																				
Outer wall			1.100					1.104					1.309					1.345		
2	1.227	1.089	1.099	50.4	0.399	1.162	1.085	1.095	4.5	0.292	1.495	1.175	1.309	53.1	0.443	1.436	1.167	1.339	5.0	0.318
3	1.223	1.080	1.096	43.0	.399	1.180	1.078	1.093	2.2	.331	1.508	1.167	1.303	46.6	.458	1.446	1.164	1.339	7.4	.333
4	1.227	1.068	1.091	35.6	.413	1.186	1.073	1.093	1.3	.344	1.515	1.158	1.299	43.0	.474	1.475	1.159	1.341	5.0	.371
5	1.227	1.066	1.085	35.8	.425	1.189	1.067	1.094	1.6	.364	1.518	1.149	1.295	41.9	.481	1.479	1.152	1.342	4.1	.378
6	1.225	1.065	1.079	36.5	.430	1.211	1.065	1.095	2.2	.383	1.511	1.142	1.286	41.2	.483	1.491	1.146	1.345	4.3	.388
7	1.210	1.063	1.068	38.0	.427	1.206	1.061	1.099	2.2	.387	1.502	1.136	1.277	41.6	.487	1.494	1.138	1.343	3.8	.393
8	1.211	1.060	1.053	40.5	.452	1.205	1.060	1.102	3.6	.359	1.501	1.131	1.285	45.7	.501	1.486	1.130	1.344	4.3	.381
9	1.214	1.059	1.047	42.5	.464	1.208	1.058	1.105	3.4	.356	1.494	1.128	1.258	45.5	.501	1.480	1.128	1.344	4.0	.374
10	1.207	1.059	1.040	43.7	.467	1.202	1.058	1.106	2.2	.348	1.480	1.127	1.250	48.3	.507	1.479	1.128	1.344	4.1	.375
11	1.210	1.059	1.034	46.1	.479	1.200	1.057	1.106	2.3	.344	1.490	1.127	1.247	48.8	.511	1.485	1.129	1.342	5.4	.385
12	1.217	1.062	1.031	49.7	.492	1.193	1.060	1.106	3.1	.330	1.497	1.151	1.243	49.5	.522	1.476	1.132	1.340	5.6	.377
Exhaust-nozzle setting, 106; bleed closed; $w\sqrt{\theta}/\delta$, 40.13 lb/sec																				
Outer wall			1.106					1.107					1.311					1.383		
2	1.243	1.099	1.103	56.3	0.416	1.159	1.091	1.093	1.8	0.291	1.505	1.187	1.311	58.1	0.449	1.443	1.176	1.346	5.9	0.318
3	1.237	1.091	1.102	50.9	.410	1.161	1.082	1.089	3.4	.304	1.495	1.177	1.310	52.7	.459	1.467	1.174	1.346	7.7	.354
4	1.229	1.074	1.098	39.8	.404	1.167	1.077	1.087	4.3	.320	1.496	1.166	1.306	47.5	.445	1.478	1.167	1.346	6.3	.369
5	1.230	1.068	1.084	37.6	.413	1.182	1.070	1.085	4.5	.350	1.505	1.157	1.304	45.4	.457	1.482	1.160	1.345	5.6	.378
6	1.225	1.066	1.069	37.5	.414	1.199	1.067	1.088	5.6	.374	1.506	1.149	1.300	44.6	.464	1.492	1.153	1.345	5.2	.387
7	1.222	1.064	1.076	39.2	.417	1.211	1.063	1.098	5.2	.380	1.506	1.138	1.288	43.9	.476	1.498	1.140	1.352	4.7	.387
8	1.216	1.061	1.069	41.8	.449	1.207	1.061	1.104	4.7	.359	1.510	1.134	1.274	45.7	.499	1.491	1.132	1.352	4.9	.377
9	1.218	1.060	1.062	43.4	.462	1.207	1.059	1.106	4.0	.355	1.504	1.130	1.264	47.0	.504	1.489	1.131	1.352	4.7	.374
10	1.214	1.059	1.043	45.2	.470	1.205	1.057	1.108	2.7	.348	1.482	1.126	1.256	47.7	.507	1.490	1.130	1.352	5.0	.376
11	1.215	1.060	1.038	47.3	.479	1.206	1.058	1.108	2.7	.351	1.498	1.126	1.251	48.8	.512	1.492	1.132	1.351	5.4	.380
12	1.220	1.062	1.032	50.4	.485	1.201	1.061	1.108	5.6	.345	1.497	1.130	1.246	51.1	.519	1.484	1.134	1.348	6.1	.373
Exhaust-nozzle setting, 30; bleed closed; $w\sqrt{\theta}/\delta$, 40.21 lb/sec																				
Outer wall			1.108					1.107					1.303					1.354		
2	1.244	1.094	1.104	55.8	0.417	1.170	1.086	1.105	1.1	0.275	1.506	1.184	1.300	55.2	0.462	1.437	1.170	1.354	5.4	0.292
3	1.237	1.088	1.102	48.2	.409	1.169	1.079	1.105	2.3	.280	1.504	1.176	1.298	49.6	.464	1.450	1.169	1.354	7.7	.313
4	1.230	1.074	1.099	38.9	.404	1.169	1.074	1.102	5.2	.265	1.511	1.171	1.295	45.1	.475	1.472	1.162	1.354	5.6	.347
5	1.229	1.067	1.094	34.2	.411	1.179	1.068	1.100	3.6	.311	1.511	1.156	1.290	43.1	.490	1.472	1.157	1.354	4.3	.348
6	1.225	1.065	1.090	36.3	.412	1.200	1.065	1.100	2.8	.354	1.510	1.146	1.284	42.2	.487	1.481	1.152	1.354	3.6	.360
7	1.222	1.063	1.080	37.8	.425	1.210	1.060	1.100	2.7	.395	1.506	1.139	1.275	41.1	.497	1.502	1.136	1.355	3.5	.387
8	1.218	1.069	1.066	40.1	.458	1.207	1.060	1.102	3.3	.365	1.506	1.131	1.259	43.5	.513	1.495	1.130	1.358	3.2	.374
9	1.218	1.060	1.069	42.0	.449	1.207	1.056	1.106	2.9	.360	1.501	1.130	1.250	44.4	.518	1.495	1.129	1.357	2.7	.374
10	1.215	1.069	1.060	43.4	.461	1.206	1.057	1.107	1.7	.355	1.501	1.130	1.255	44.8	.527	1.496	1.130	1.356	2.6	.377
11	1.214	1.062	1.044	45.7	.469	1.202	1.057	1.107	2.1	.349	1.503	1.132	1.238	45.6	.534	1.496	1.131	1.356	4.1	.377
12	1.219	1.065	1.058	46.3	.464	1.197	1.059	1.107	7.2	.340	1.509	1.135	1.252	46.8	.548	1.496	1.130	1.356	4.8	.383
Exhaust-nozzle setting, 160; bleed closed; $w\sqrt{\theta}/\delta$, 39.10 lb/sec																				
Outer wall			1.104					1.104					1.288					1.352		
2	1.254	1.099	1.105	56.7	0.429	1.168	1.087	1.101	-4.8	0.293	1.508	1.192	1.297	58.0	0.470	1.438	1.174	1.351	5.2	0.295
3	1.243	1.092	1.105	55.2	.413	1.148	1.077	1.097	0	.254	1.498	1.183	1.294	53.2	.462	1.445	1.168	1.350	6.9	.313
4	1.226	1.077	1.103	42.5	.382	1.160	1.070	1.096	1.9	.288	1.499	1.173	1.291	47.6	.467	1.456	1.160	1.349	5.4	.332
5	1.228	1.068	1.100	37.5	.401	1.164	1.066	1.093	3.8	.300	1.506	1.162	1.287	44.1	.478	1.455	1.155	1.349	4.8	.352
6	1.225	1.066	1.096	37.0	.409	1.178	1.062	1.092	3.9	.350	1.506	1.152	1.280	43.3	.487	1.463	1.148	1.348	4.5	.344
7	1.219	1.065	1.095	38.2	.412	1.203	1.060	1.095	3.1	.375	1.504	1.140	1.268	41.7	.489	1.467	1.138	1.349	4.0	.376
8	1.218	1.069	1.072	40.2	.450	1.203	1.060	1.098	3.5	.381	1.507	1.131	1.253	43.0	.520	1.486	1.131	1.349	3.7	.374
9	1.216	1.065	1.067	42.2	.437	1.207	1.068	1.103	2.8	.361	1.502	1.126	1.244	44.1	.525	1.488	1.130	1.352	3.2	.372
10	1.210	1.066	1.060	45.4	.438	1.206	1.068	1.104	2.5	.361	1.498	1.127	1.237	44.4	.530	1.469	1.130	1.351	3.3	.376
11	1.214	1.068	1.066	45.9	.459	1.204	1.053	1.105	1.7	.357	1.500	1.128	1.232	46.2	.536	1.488	1.126	1.353	4.4	.371
12	1.222	1.069	1.062	46.3	.466	1.197	1.060	1.106	3.4	.359	1.509	1.132	1.227	46.4	.552	1.481	1.130	1.352	5.3	.383

Negative angles signify turning past axial direction.

[redacted]

TABLE II. - Continued. RADIAL DISTRIBUTION OF PERFORMANCE DATA FROM FIVE-STAGE TRANSONIC COMPRESSOR

(a) Continued. Series 1.

2. Speed, 80-percent design.

Radial position	Station 3					Station 4					Station 5					Station 6				
	P_3/P_2	T_3/T_2	p_3/P_2	β, deg	M	P_4/P_2	T_4/T_2	p_4/P_2	β, deg	M	P_5/P_2	T_5/T_2	p_5/P_2	β, deg	M	P_6/P_2	T_6/T_2	p_6/P_2	β, deg	M
Exhaust-nozzle setting, 0; bleed open; $w\sqrt{\theta}/\delta$, 51.77 lb/sec																				
Outer wall			1.114					1.119					1.406					1.456		
2	1.286	1.101	1.113	41.2	0.460	1.217	1.098	1.112	2.3	0.361	1.678	1.214	1.404	46.6	0.512	1.591	1.206	1.446	4.9	0.372
3	1.299	1.093	1.110	35.8	.479	1.275	1.093	1.112	2.0	.446	1.705	1.206	1.400	39.4	.538	1.635	1.203	1.450	6.5	.418
4	1.300	1.084	1.104	33.1	.489	1.279	1.087	1.109	1.6	.457	1.718	1.200	1.396	37.1	.552	1.687	1.197	1.443	6.1	.478
5	1.292	1.081	1.098	33.3	.487	1.285	1.084	1.110	.5	.462	1.708	1.188	1.390	37.3	.550	1.692	1.190	1.449	5.6	.476
6	1.287	1.082	1.094	34.2	.487	1.281	1.080	1.113	.4	.452	1.693	1.181	1.385	37.6	.545	1.686	1.181	1.454	4.1	.465
7	1.280	1.081	1.081	36.2	.497	1.274	1.079	1.117	1.8	.438	1.678	1.178	1.368	39.6	.549	1.669	1.173	1.456	3.8	.446
8	1.274	1.077	1.064	39.4	.514	1.267	1.075	1.120	3.1	.425	1.678	1.172	1.349	43.0	.568	1.651	1.169	1.455	4.8	.432
9	1.269	1.077	1.054	41.2	.522	1.263	1.074	1.124	2.7	.412	1.672	1.168	1.338	43.7	.573	1.645	1.168	1.454	4.5	.424
10	1.269	1.075	1.042	42.7	.538	1.261	1.072	1.125	2.0	.407	1.664	1.166	1.328	45.2	.577	1.638	1.168	1.457	4.7	.413
11	1.280	1.078	1.052	45.7	.562	1.264	1.074	1.127	2.7	.408	1.662	1.168	1.322	46.8	.582	1.647	1.170	1.455	5.6	.427
12	1.288	1.082	1.025	48.2	.580	1.261	1.079	1.128	3.8	.403	1.668	1.172	1.318	49.5	.592	1.642	1.172	1.450	6.1	.425
Exhaust-nozzle setting, 180; bleed closed; $w\sqrt{\theta}/\delta$, 49.93 lb/sec																				
Outer wall			1.127					1.134					1.414					1.476		
2	1.290	1.104	1.126	44.1	0.445	1.226	1.102	1.120	3.6	0.361	1.698	1.217	1.410	49.3	0.520	1.600	1.212	1.472	1.3	0.347
3	1.300	1.093	1.124	39.1	.461	1.259	1.096	1.121	3.1	.380	1.718	1.208	1.405	43.7	.544	1.630	1.212	1.472	2.2	.385
4	1.303	1.084	1.119	34.1	.471	1.266	1.088	1.119	2.6	.424	1.729	1.199	1.401	40.1	.557	1.666	1.200	1.473	3.2	.422
5	1.296	1.082	1.114	33.8	.470	1.276	1.084	1.121	1.8	.435	1.717	1.190	1.394	39.6	.554	1.674	1.193	1.474	4.5	.431
6	1.291	1.081	1.109	34.2	.471	1.278	1.081	1.122	1.1	.436	1.707	1.182	1.384	39.4	.556	1.687	1.184	1.473	2.7	.444
7	1.287	1.078	1.097	36.0	.483	1.268	1.078	1.128	1.8	.412	1.695	1.176	1.374	40.9	.556	1.675	1.176	1.478	1.8	.427
8	1.278	1.076	1.081	38.9	.495	1.265	1.076	1.131	4.4	.404	1.685	1.170	1.354	44.5	.568	1.653	1.170	1.478	5.0	.403
9	1.275	1.075	1.072	40.4	.504	1.268	1.073	1.134	5.4	.402	1.681	1.167	1.344	45.9	.575	1.651	1.168	1.480	4.9	.399
10	1.272	1.074	1.061	42.6	.516	1.260	1.072	1.135	5.9	.389	1.676	1.165	1.334	46.6	.580	1.659	1.168	1.478	4.9	.409
11	1.278	1.075	1.061	44.9	.536	1.268	1.075	1.136	5.9	.399	1.678	1.167	1.327	47.3	.589	1.662	1.167	1.478	5.6	.412
12	1.288	1.077	1.043	47.2	.557	1.256	1.077	1.138	5.8	.346	1.683	1.171	1.317	50.2	.602	1.642	1.170	1.476	7.4	.393
Exhaust-nozzle setting, 120; bleed closed; $w\sqrt{\theta}/\delta$, 50.44 lb/sec																				
Outer wall			1.128					1.132					1.415					1.477		
2	1.292	1.099	1.126	42.6	0.447	1.225	1.100	1.119	6.2	0.362	1.701	1.213	1.411	48.8	0.524	1.595	1.210	1.471	5.2	0.342
3	1.304	1.089	1.124	37.0	.466	1.261	1.094	1.117	5.5	.420	1.723	1.206	1.407	42.8	.546	1.634	1.207	1.472	7.0	.389
4	1.306	1.080	1.119	33.7	.476	1.268	1.088	1.117	4.5	.428	1.730	1.195	1.403	40.4	.556	1.681	1.200	1.474	5.5	.438
5	1.299	1.079	1.112	34.0	.476	1.275	1.086	1.119	3.7	.435	1.719	1.187	1.396	39.4	.554	1.688	1.197	1.476	4.7	.443
6	1.293	1.078	1.107	34.9	.477	1.279	1.085	1.121	3.7	.438	1.703	1.180	1.389	39.5	.548	1.693	1.182	1.480	3.9	.442
7	1.285	1.076	1.094	36.9	.485	1.271	1.077	1.125	4.9	.422	1.694	1.173	1.374	41.4	.556	1.679	1.174	1.481	3.6	.427
8	1.278	1.075	1.077	39.8	.500	1.268	1.075	1.129	5.6	.411	1.688	1.168	1.355	44.9	.569	1.666	1.169	1.485	4.2	.409
9	1.275	1.074	1.069	41.0	.509	1.265	1.075	1.132	5.2	.402	1.683	1.168	1.344	45.8	.576	1.666	1.170	1.484	4.0	.409
10	1.273	1.073	1.057	42.5	.522	1.257	1.076	1.132	4.8	.389	1.681	1.165	1.332	46.8	.586	1.660	1.170	1.483	4.1	.404
11	1.289	1.073	1.048	45.5	.552	1.265	1.078	1.134	6.0	.398	1.684	1.165	1.324	47.5	.596	1.669	1.170	1.482	5.2	.416
12	1.289	1.078	1.042	48.7	.560	1.253	1.078	1.135	4.7	.378	1.686	1.171	1.316	50.4	.606	1.667	1.172	1.482	6.2	.413

TABLE II. - Continued. RADIAL DISTRIBUTION OF PERFORMANCE DATA FROM FIVE-STAGE TRANSONIC COMPRESSOR

(a) Continued. Series 1.

2. Concluded. Speed, 80-percent design.

Radial position	Station 3					Station 4					Station 5					Station 6				
	P_3/P_2	T_3/T_2	p_3/P_2	β, deg	M	P_4/P_2	T_4/T_2	p_4/P_2	β, deg	M	P_5/P_2	T_5/T_2	p_5/P_2	β, deg	M	P_6/P_2	T_6/T_2	p_6/P_2	β, deg	M
Exhaust-nozzle setting, 300; bleed closed; $w\sqrt{\theta}/\delta$, 47.46 lb/sec																				
Outer wall			1.130					1.136					1.416					1.489		
2	1.303	1.116	1.130	53.2	0.457	1.224	1.112	1.136	2.9	0.328	1.711	1.238	1.413	56.6	0.551	1.606	1.227	1.488	6.6	0.331
3	1.301	1.105	1.129	45.3	.455	1.232	1.102	1.134	2.6	.346	1.706	1.227	1.408	50.3	.551	1.618	1.218	1.488	8.4	.348
4	1.304	1.091	1.127	37.8	.461	1.235	1.094	1.132	2.6	.356	1.706	1.217	1.402	46.0	.537	1.639	1.210	1.487	6.6	.376
5	1.305	1.090	1.125	36.8	.466	1.254	1.088	1.129	3.4	.390	1.710	1.202	1.394	43.8	.547	1.647	1.204	1.487	5.3	.385
6	1.303	1.086	1.121	36.4	.469	1.271	1.085	1.128	3.7	.416	1.704	1.194	1.386	43.0	.552	1.652	1.195	1.487	5.0	.391
7	1.297	1.082	1.111	38.2	.475	1.280	1.079	1.127	4.3	.430	1.699	1.180	1.369	42.8	.564	1.675	1.180	1.488	4.5	.415
8	1.286	1.078	1.095	40.4	.484	1.265	1.077	1.134	3.9	.398	1.694	1.173	1.349	44.6	.579	1.669	1.173	1.490	3.8	.406
9	1.280	1.075	1.088	42.1	.488	1.270	1.075	1.135	3.7	.404	1.686	1.167	1.337	46.3	.586	1.657	1.170	1.490	3.5	.392
10	1.276	1.073	1.078	43.4	.498	1.262	1.073	1.139	3.2	.386	1.686	1.165	1.325	46.9	.597	1.667	1.169	1.490	3.6	.403
11	1.286	1.071	1.070	46.6	.519	1.267	1.075	1.139	3.6	.393	1.687	1.164	1.317	48.0	.605	1.669	1.171	1.490	5.0	.406
12	1.292	1.078	1.065	49.0	.534	1.273	1.079	1.136	3.4	.403	1.687	1.173	1.308	50.4	.614	1.662	1.176	1.490	5.9	.398
Exhaust-nozzle setting, 240; bleed closed; $w\sqrt{\theta}/\delta$, 49.69 lb/sec																				
Outer wall			1.128					1.137					1.417					1.488		
2	1.297	1.103	1.124	42.8	0.456	1.233	1.101	1.134	2.7	0.347	1.704	1.220	1.412	50.0	0.525	1.619	1.212	1.489	4.2	0.348
3	1.303	1.095	1.121	36.6	.469	1.256	1.093	1.133	2.5	.388	1.719	1.213	1.408	45.1	.542	1.628	1.210	1.486	5.2	.364
4	1.306	1.084	1.119	34.2	.474	1.267	1.085	1.131	1.4	.406	1.728	1.203	1.403	42.2	.554	1.667	1.202	1.487	3.7	.408
5	1.293	1.084	1.116	34.0	.464	1.280	1.079	1.130	.7	.426	1.729	1.197	1.396	40.5	.561	1.676	1.194	1.490	3.1	.414
6	1.289	1.080	1.110	34.4	.466	1.282	1.075	1.130	.6	.428	1.713	1.184	1.388	40.0	.557	1.691	1.181	1.492	2.0	.427
7	1.286	1.075	1.106	36.6	.470	1.276	1.073	1.132	1.4	.417	1.702	1.176	1.371	41.2	.565	1.684	1.173	1.491	1.5	.421
8	1.282	1.078	1.095	39.5	.480	1.274	1.070	1.139	2.6	.403	1.694	1.170	1.351	44.6	.577	1.671	1.166	1.494	2.3	.403
9	1.278	1.076	1.081	40.7	.494	1.271	1.072	1.140	2.1	.398	1.687	1.165	1.339	45.7	.584	1.669	1.164	1.492	1.7	.403
10	1.273	1.074	1.074	41.9	.498	1.265	1.068	1.141	1.7	.387	1.684	1.165	1.328	46.9	.593	1.668	1.164	1.494	2.4	.399
11	1.268	1.076	1.066	44.8	.505	1.271	1.072	1.141	2.6	.396	1.682	1.165	1.321	47.9	.598	1.678	1.167	1.490	3.3	.416
12	1.265	1.074	1.059	46.0	.511	1.270	1.072	1.141	2.8	.394	1.681	1.167	1.314	50.6	.603	1.666	1.164	1.489	3.5	.404

[redacted]

TABLE II. - Continued. RADIAL DISTRIBUTION OF PERFORMANCE DATA FROM FIVE-STAGE TRANSONIC COMPRESSOR

(a) Continued. Series 1.

3. Speed, 90-percent design.

Radial position	Station 3					Station 4					Station 5					Station 6				
	P_3/P_2	T_3/T_2	p_3/P_2	β, deg	M	P_4/P_2	T_4/T_2	p_4/P_2	β, deg	M	P_5/P_2	T_5/T_2	p_5/P_2	β, deg	M	P_6/P_2	T_6/T_2	p_6/P_2	β, deg	M
Exhaust-nozzle setting, 0; bleed open; $w\sqrt{\theta}/\delta$, 63.35 lb/sec																				
Outer wall			1.110					1.102					1.498					1.554		
2	1.333	1.127	1.106	41.0	0.523	1.251	1.123	1.089	1.8	0.449	1.859	1.269	1.496	45.8	0.566	1.746	1.261	1.540	4.6	0.428
3	1.374	1.115	1.103	33.0	.570	1.343	1.114	1.091	1.8	.552	1.922	1.259	1.494	38.9	.611	1.806	1.255	1.539	6.8	.484
4	1.379	1.107	1.097	30.5	.581	1.354	1.106	1.093	1.8	.562	1.953	1.246	1.491	35.9	.633	1.887	1.246	1.540	6.2	.546
5	1.367	1.100	1.090	30.6	.577	1.361	1.098	1.100	.1	.561	1.938	1.233	1.485	35.2	.629	1.903	1.235	1.545	5.0	.553
6	1.352	1.096	1.085	30.6	.570	1.354	1.094	1.103	-1.2	.549	1.915	1.222	1.476	35.8	.621	1.896	1.222	1.550	3.1	.544
7	1.339	1.092	1.071	32.6	.574	1.333	1.090	1.101	-.2	.530	1.882	1.213	1.458	38.2	.615	1.860	1.211	1.557	2.3	.511
8	1.344	1.092	1.052	35.6	.602	1.334	1.090	1.106	1.8	.525	1.868	1.208	1.433	42.0	.627	1.844	1.208	1.555	4.0	.499
9	1.344	1.092	1.042	37.7	.615	1.334	1.090	1.108	1.8	.522	1.857	1.207	1.417	43.2	.634	1.831	1.206	1.557	3.2	.487
10	1.341	1.092	1.027	39.8	.629	1.333	1.091	1.110	1.4	.518	1.850	1.205	1.404	44.5	.640	1.826	1.206	1.552	3.7	.487
11	1.339	1.092	1.016	42.5	.640	1.328	1.092	1.110	1.3	.512	1.847	1.207	1.395	45.4	.646	1.839	1.209	1.558	4.5	.492
12	1.357	1.099	1.008	45.5	.666	1.315	1.096	1.115	1.4	.494	1.851	1.215	1.386	48.7	.656	1.836	1.213	1.557	4.9	.491
Exhaust-nozzle setting, 153; bleed closed; $w\sqrt{\theta}/\delta$, 62.40 lb/sec																				
Outer wall			1.126					1.129					1.533					1.607		
2	1.363	1.128	1.123	41.5	0.533	1.292	1.126	1.112	3.4	0.456	1.913	1.274	1.529	47.0	0.575	1.784	1.265	1.585	4.7	0.424
3	1.392	1.116	1.120	33.8	.566	1.366	1.116	1.115	.5	.548	1.957	1.263	1.526	41.0	.607	1.848	1.260	1.583	6.7	.475
4	1.399	1.103	1.113	31.1	.582	1.376	1.108	1.113	0	.559	1.968	1.250	1.521	37.4	.618	1.918	1.250	1.583	5.6	.531
5	1.388	1.103	1.106	30.9	.579	1.376	1.100	1.121	-1.0	.549	1.963	1.239	1.514	37.3	.621	1.924	1.239	1.589	4.3	.530
6	1.372	1.098	1.100	31.3	.571	1.365	1.095	1.125	-1.8	.533	1.941	1.228	1.504	37.4	.614	1.918	1.228	1.595	2.5	.520
7	1.353	1.098	1.086	32.8	.569	1.344	1.091	1.125	-1.6	.509	1.925	1.221	1.485	40.0	.620	1.888	1.214	1.596	1.9	.496
8	1.351	1.094	1.067	36.3	.590	1.341	1.092	1.130	-.7	.502	1.902	1.216	1.459	43.5	.627	1.868	1.213	1.600	3.2	.476
9	1.353	1.093	1.055	38.2	.606	1.339	1.092	1.133	-.8	.494	1.882	1.210	1.443	44.9	.629	1.860	1.211	1.596	2.9	.472
10	1.354	1.094	1.042	40.2	.624	1.335	1.093	1.134	-1.0	.489	1.872	1.209	1.427	45.8	.634	1.860	1.210	1.596	3.0	.473
11	1.354	1.096	1.030	43.2	.638	1.335	1.094	1.136	-.8	.485	1.877	1.211	1.419	46.9	.645	1.866	1.214	1.595	4.2	.479
12	1.370	1.103	1.021	47.0	.662	1.327	1.096	1.143	-.2	.487	1.889	1.219	1.410	49.8	.660	1.857	1.217	1.597	4.7	.475
Exhaust-nozzle setting, 75; bleed closed; $w\sqrt{\theta}/\delta$, 61.90 lb/sec																				
Outer wall			1.137					1.129					1.525					1.593		
2	1.367	1.129	1.131	41.3	0.528	1.286	1.122	1.116	2.8	0.441	1.910	1.266	1.520	47.2	0.580	1.777	1.255	1.592	3.8	0.399
3	1.398	1.113	1.128	34.4	.561	1.361	1.111	1.116	2.9	.536	1.937	1.255	1.513	40.4	.605	1.829	1.249	1.593	5.6	.449
4	1.398	1.103	1.121	31.0	.569	1.370	1.105	1.116	2.0	.548	1.968	1.244	1.507	37.8	.630	1.908	1.244	1.594	5.2	.514
5	1.381	1.097	1.115	31.7	.562	1.369	1.096	1.118	.8	.544	1.948	1.232	1.498	38.3	.625	1.915	1.233	1.598	3.7	.516
6	1.369	1.096	1.109	32.2	.558	1.359	1.092	1.121	-.1	.531	1.916	1.221	1.488	38.1	.612	1.908	1.221	1.602	1.9	.506
7	1.353	1.094	1.093	33.4	.554	1.340	1.089	1.127	.6	.504	1.897	1.213	1.470	39.9	.614	1.884	1.210	1.604	1.5	.485
8	1.348	1.092	1.075	37.2	.578	1.335	1.087	1.130	2.0	.498	1.876	1.208	1.447	43.6	.621	1.862	1.206	1.606	2.4	.465
9	1.344	1.090	1.065	38.2	.587	1.338	1.086	1.131	2.0	.498	1.858	1.204	1.433	45.0	.621	1.850	1.204	1.602	2.1	.458
10	1.341	1.093	1.051	40.4	.600	1.330	1.087	1.134	1.5	.486	1.859	1.204	1.418	45.5	.634	1.855	1.204	1.603	2.4	.463
11	1.344	1.093	1.038	43.5	.618	1.330	1.090	1.136	1.9	.483	1.864	1.209	1.409	46.6	.645	1.854	1.206	1.599	3.0	.465
12	1.362	1.099	1.029	47.1	.646	1.317	1.095	1.140	2.6	.466	1.878	1.216	1.397	49.6	.664	1.858	1.211	1.599	4.7	.468

Negative angles signify turning past axial direction.

[redacted]

TABLE II. - Continued. RADIAL DISTRIBUTION OF PERFORMANCE DATA FROM FIVE-STAGE TRANSONIC COMPRESSOR

(a) Continued. Series 1.

3. Concluded. Speed, 90-percent design.

Radial position	Station 3					Station 4					Station 5					Station 6				
	P_3/P_2	T_3/T_2	p_3/P_2	β, deg	M	P_4/P_2	T_4/T_2	p_4/P_2	β, deg	M	P_5/P_2	T_5/T_2	p_5/P_2	β, deg	M	P_6/P_2	T_6/T_2	p_6/P_2	β, deg	M
Exhaust-nozzle setting, 330; bleed closed; $w\sqrt{\theta}/\delta$, 59.36 lb/sec																				
Outer wall			1.162					1.171					1.584					1.672		
2	1.407	1.144	1.161	42.1	0.531	1.325	1.131	1.167	2.9	0.430	1.972	1.281	1.579	48.6	0.573	1.850	1.273	1.671	2.6	0.384
3	1.423	1.128	1.160	34.7	.549	1.378	1.122	1.163	2.0	.499	1.999	1.271	1.572	41.8	.597	1.878	1.270	1.671	4.9	.412
4	1.429	1.114	1.155	31.0	.560	1.390	1.112	1.160	.6	.515	2.013	1.259	1.565	39.1	.611	1.950	1.258	1.670	3.1	.475
5	1.409	1.110	1.150	30.8	.547	1.398	1.102	1.157	0	.525	2.002	1.247	1.554	39.2	.612	1.944	1.248	1.670	2.2	.472
6	1.392	1.104	1.143	31.4	.537	1.386	1.100	1.157	-.7	.515	1.971	1.236	1.544	38.8	.602	1.952	1.234	1.668	.8	.480
7	1.365	1.102	1.130	34.0	.526	1.364	1.094	1.158	-.2	.490	1.934	1.225	1.524	42.7	.594	1.918	1.224	1.665	0	.454
8	1.355	1.096	1.111	37.3	.540	1.351	1.092	1.161	1.4	.471	1.911	1.217	1.499	45.6	.600	1.878	1.220	1.666	1.6	.418
9	1.351	1.094	1.100	39.4	.549	1.346	1.090	1.164	1.4	.459	1.906	1.215	1.484	46.6	.609	1.876	1.216	1.661	.7	.420
10	1.348	1.094	1.087	41.3	.563	1.339	1.092	1.166	.5	.450	1.903	1.211	1.470	47.6	.619	1.878	1.218	1.660	1.8	.423
11	1.357	1.100	1.078	43.9	.582	1.337	1.090	1.167	1.8	.445	1.899	1.215	1.458	49.1	.626	1.880	1.216	1.656	2.4	.429
12	1.374	1.102	1.071	46.9	.608	1.336	1.098	1.168	6.4	.441	1.917	1.221	1.447	52.4	.647	1.867	1.220	1.658	3.0	.414
Exhaust-nozzle setting, 240; bleed closed; $w\sqrt{\theta}/\delta$, 61.65 lb/sec																				
Outer wall			1.138					1.142					1.562					1.634		
2	1.384	1.130	1.135	41.0	0.540	1.303	1.124	1.142	2.9	0.438	1.931	1.272	1.562	48.0	0.559	1.811	1.260	1.634	3.6	0.386
3	1.402	1.115	1.132	33.4	.561	1.374	1.112	1.143	2.1	.518	1.977	1.257	1.558	41.4	.593	1.868	1.260	1.634	4.8	.442
4	1.408	1.101	1.126	30.5	.574	1.380	1.104	1.143	1.6	.525	1.999	1.248	1.555	38.7	.610	1.937	1.245	1.633	4.6	.499
5	1.398	1.099	1.120	29.9	.572	1.392	1.097	1.144	0	.537	1.982	1.238	1.548	38.1	.604	1.948	1.235	1.633	3.0	.508
6	1.386	1.092	1.113	30.8	.568	1.378	1.094	1.144	-.6	.523	1.947	1.226	1.540	37.6	.589	1.938	1.227	1.632	.9	.501
7	1.361	1.088	1.099	32.8	.561	1.358	1.085	1.143	0	.502	1.930	1.212	1.521	39.8	.593	1.904	1.208	1.631	.4	.475
8	1.358	1.090	1.080	36.3	.582	1.347	1.088	1.140	1.4	.494	1.898	1.210	1.498	43.8	.590	1.870	1.208	1.629	-.7	.448
9	1.352	1.088	1.070	38.1	.588	1.342	1.088	1.139	1.8	.490	1.886	1.201	1.485	45.1	.595	1.858	1.206	1.629	2.3	.438
10	1.347	1.088	1.058	39.9	.599	1.330	1.083	1.137	1.5	.478	1.882	1.204	1.471	46.3	.603	1.856	1.199	1.628	2.1	.437
11	1.360	1.090	1.046	42.5	.624	1.360	1.071	1.136	---	.514	1.881	1.204	1.463	47.0	.610	1.894	1.202	1.627	2.9	.470
12	1.378	1.092	1.039	45.4	.648	1.364	1.081	1.136	---	.518	1.901	1.214	1.455	50.6	.630	1.880	1.210	1.627	4.1	.460

Negative angles signify turning past axial direction.

TABLE II. - Continued. RADIAL DISTRIBUTION OF PERFORMANCE DATA FROM FIVE-STAGE TRANSONIC COMPRESSOR

(a) Concluded. Series 1.

4. Speed, 100-percent design.

Radial position	Station 3					Station 4					Station 5					Station 6				
	P_3/P_2	T_3/T_2	p_3/P_2	β, deg	M	P_4/P_2	T_4/T_2	p_4/P_2	β, deg	M	P_5/P_2	T_5/T_2	p_5/P_2	β, deg	M	P_6/P_2	T_6/T_2	p_6/P_2	β, deg	M
Exhaust-nozzle setting, 0; bleed open; $w\sqrt{\theta}/\delta$, 69.89 lb/sec																				
Outer wall			0.989					1.016					1.407					1.500		
2	1.185	1.141	.996	42.7	0.504	1.154	1.113	1.018	-1.8	0.427	1.776	1.315	1.413	51.4	0.581	1.676	1.285	1.501	0.9	0.400
3	1.234	1.122	1.004	26.4	.551	1.223	1.106	1.020	-2.2	.516	1.844	1.289	1.416	39.6	.624	1.723	1.280	1.502	1.9	.447
4	1.302	1.105	1.015	22.8	.607	1.266	1.098	1.023	-2.3	.560	1.906	1.285	1.422	35.9	.660	1.828	1.273	1.506	.9	.535
5	1.332	1.109	1.020	25.1	.629	1.306	1.096	1.027	-1.2	.596	1.956	1.274	1.427	35.4	.674	1.865	1.264	1.507	.5	.580
6	1.352	1.113	1.024	25.0	.645	1.329	1.088	1.030	-1.3	.614	1.966	1.268	1.431	35.3	.690	1.913	1.258	1.512	0	.590
7	1.417	1.111	1.025	27.8	.696	1.385	1.086	1.046	-.4	.646	2.001	1.263	1.434	36.2	.707	1.957	1.251	1.525	0	.610
8	1.422	1.107	1.020	29.7	.707	1.400	1.096	1.057	.2	.647	2.028	1.251	1.430	35.9	.724	1.986	1.234	1.531	0	.621
9	1.418	1.108	1.015	31.0	.706	1.398	1.096	1.062	.3	.658	2.041	1.487	1.422	37.4	.738	1.985	1.238	1.536	-.2	.617
10	1.409	1.106	1.009	32.2	.708	1.389	1.098	1.062	.2	.631	2.026	1.236	1.414	38.8	.736	1.971	1.234	1.535	-.1	.608
11	1.405	1.102	1.005	34.9	.709	1.382	1.096	1.064	-.1	.622	1.999	1.238	1.404	39.9	.728	1.949	1.234	1.534	.7	.595
12	1.412	1.112	.998	38.5	.721	1.356	1.102	1.089	-.3	.595	1.897	1.244	1.394	43.2	.736	1.901	1.240	1.534	1.5	.562
Exhaust-nozzle setting, 180; bleed closed; $w\sqrt{\theta}/\delta$, 69.99 lb/sec																				
Outer wall			0.998					1.024					1.443					1.558		
2	1.197	1.132	.998	45.5	0.516	1.167	1.123	1.025	-1.5	0.438	1.845	1.317	1.445	53.7	0.605	1.727	1.307	1.560	0.8	0.383
3	1.246	1.114	1.001	29.6	.570	1.240	1.122	1.023	-1.7	.531	1.904	1.303	1.444	41.7	.641	1.770	1.304	1.562	2.2	.426
4	1.306	1.104	1.006	25.4	.624	1.284	1.112	1.026	-1.5	.577	1.967	1.291	1.446	37.2	.677	1.879	1.293	1.566	1.7	.517
5	1.344	1.110	1.010	26.2	.652	1.325	1.112	1.030	-.6	.610	1.989	1.279	1.449	36.9	.686	1.911	1.285	1.570	1.7	.537
6	1.359	1.108	1.014	27.4	.660	1.340	1.110	1.037	-.8	.616	2.022	1.269	1.454	36.9	.704	1.961	1.278	1.576	1.9	.568
7	1.427	1.117	1.019	29.5	.711	1.399	1.114	1.053	.5	.650	2.046	1.265	1.462	37.1	.710	2.017	1.265	1.588	2.1	.597
8	1.435	1.108	1.015	32.1	.722	1.409	1.112	1.066	.6	.644	2.057	1.251	1.469	37.0	.710	2.020	1.257	1.596	.2	.590
9	1.425	1.108	1.010	33.6	.719	1.401	1.109	1.070	0	.633	2.054	1.245	1.470	39.1	.706	1.998	1.253	1.596	-.5	.576
10	1.414	1.106	1.002	35.1	.718	1.397	1.107	1.069	.4	.650	2.048	1.241	1.460	40.5	.712	1.992	1.249	1.597	.6	.571
11	1.407	1.110	.996	37.7	.720	1.396	1.111	1.069	.4	.629	2.092	1.241	1.455	41.2	.702	1.991	1.257	1.595	1.4	.572
12	1.423	1.119	.991	40.6	.756	1.385	1.120	1.078	0	.608	2.018	1.255	1.452	44.6	.702	1.976	1.261	1.593	2.2	.564
Exhaust-nozzle setting, 215; bleed closed; $w\sqrt{\theta}/\delta$, 69.74 lb/sec																				
Outer wall			1.008					1.032					1.468					1.584		
2	1.213	1.146	1.010	44.4	0.519	1.179	1.126	1.032	-1.3	0.440	1.872	1.334	1.467	54.5	0.600	1.750	1.310	1.587	1.7	0.377
3	1.260	1.121	1.012	30.3	.569	[illegible]	1.120	1.034	-1.5	.524	1.929	1.315	1.466	43.3	.638	1.786	1.306	1.590	2.6	.420
4	1.314	1.111	1.015	26.0	.619	[illegible]	1.108	1.037	-1.4	.566	1.977	1.294	1.465	38.4	.666	1.906	1.293	1.593	2.2	.512
5	1.342	1.115	1.016	27.2	.643	[illegible]	1.104	1.043	-.8	.605	2.013	1.286	1.463	37.3	.691	1.939	1.281	1.596	2.3	.536
6	1.362	1.115	1.016	27.7	.660	1.351	1.104	1.047	-.6	.614	2.042	1.276	1.460	37.0	.709	1.979	1.271	1.600	2.5	.569
7	1.426	1.100	1.012	29.7	.717	1.407	1.106	1.058	.5	.651	2.061	1.246	1.455	37.5	.725	2.036	1.258	1.608	1.9	.591
8	1.427	1.115	1.005	32.6	.728	1.413	1.096	1.069	.1	.644	2.060	1.256	1.444	37.3	.730	2.012	1.242	1.610	-.3	.573
9	1.416	1.111	.996	35.5	.724	1.400	1.104	1.072	.1	.629	2.066	1.246	1.435	39.0	.736	1.996	1.242	1.613	0	.560
10	1.406	1.109	.990	35.7	.727	1.396	1.096	1.071	0	.629	2.031	1.243	1.425	40.7	.732	1.982	1.244	1.614	.6	.550
11	1.400	1.109	.984	37.7	.728	1.389	1.104	1.070	0	.622	2.012	1.247	1.413	41.7	.729	1.981	1.248	1.612	2.2	.550
12	1.415	1.117	.980	41.6	.744	1.382	1.106	1.068	-.4	.618	2.024	1.250	1.401	45.6	.745	1.976	1.250	1.607	3.1	.551
Exhaust-nozzle setting, 240; bleed closed; $w\sqrt{\theta}/\delta$, 69.67 lb/sec																				
Outer wall			1.000					1.025					1.488					1.583		
2	1.209	1.145	1.002	46.6	0.524	1.176	1.126	1.028	-0.9	0.441	1.864	1.328	1.488	54.9	0.594	1.755	1.313	1.586	1.3	0.382
3	1.258	1.124	1.006	30.6	.572	1.257	1.120	1.033	-1.3	.537	1.907	1.310	1.487	43.1	.624	1.901	1.307	1.590	2.6	.426
4	1.327	1.107	1.013	26.1	.633	1.287	1.110	1.036	-1.1	.573	1.958	1.294	1.466	39.0	.656	1.903	1.296	1.594	2.5	.509
5	1.346	1.117	1.019	27.1	.643	1.325	1.103	1.045	-1.0	.593	1.990	1.288	1.465	38.0	.676	1.942	1.282	1.600	2.2	.554
6	1.377	1.117	1.023	28.5	.666	1.349	1.106	1.050	-1.2	.609	2.036	1.280	1.462	37.3	.704	1.988	1.274	1.606	2.3	.561
7	1.441	1.117	1.030	30.3	.710	1.400	1.104	1.061	.6	.642	2.056	1.266	1.460	37.2	.718	2.025	1.262	1.617	2.1	.576
8	1.425	1.113	1.027	30.5	.700	1.408	1.104	1.070	.5	.639	2.038	1.252	1.452	37.4	.713	2.013	1.244	1.621	-.3	.565
9	1.424	1.105	1.020	34.4	.707	1.412	1.108	1.074	1.1	.637	2.040	1.240	1.444	39.6	.721	2.022	1.243	1.620	0	.572
10	1.416	1.103	1.010	35.7	.714	1.407	1.104	1.078	1.1	.628	2.023	1.238	1.434	40.8	.719	1.980	1.244	1.617	.8	.546
11	1.405	1.106	.999	38.6	.715	1.392	1.100	1.079	.8	.614	2.009	1.240	1.424	41.7	.715	1.986	1.245	1.614	.6	.552
12	1.417	1.113	.990	42.2	.734	1.374	1.102	1.081	.6	.596	2.005	1.252	1.413	45.8	.725	1.964	1.247	1.612	.5	.538

Negative angles signify turning past axial direction.

[redacted]

TABLE II. - Continued. RADIAL DISTRIBUTION OF PERFORMANCE DATA FROM FIVE-STAGE TRANSONIC COMPRESSOR

(b) Series 2.

1. Speed, 70-percent design.

Radial position	Station 7 P_7/P_2	T_7/T_2	p_7/P_2	β, deg	M	Station 8 P_8/P_2	T_8/T_2	p_8/P_2	β, deg	M	Station 9 P_9/P_2	T_9/T_2	p_9/P_2	β, deg	M	Station 10 P_{10}/P_2	T_{10}/T_2	p_{10}/P_2	β, deg	M
Exhaust-nozzle setting, 0; bleed open; $w\sqrt{\theta}/\delta$, 41.73 lb/sec																				
Outer wall			1.560					1.604					1.831					1.838		
2	1.764	1.237	1.559	42.2	0.424	1.717	1.232	1.605	-0.7	0.311	2.023	1.283	1.829	35.8	0.383	1.975	1.292	1.839	-3.8	0.322
3	1.777	1.234	1.558	38.3	.438	1.736	1.230	1.606	1.6	.335	2.059	1.290	1.828	32.9	.408	2.017	1.290	1.839	-.6	.366
4	1.791	1.231	1.556	34.8	.454	1.762	1.223	1.607	1.4	.365	2.004	1.290	1.827	30.4	.438	2.049	1.285	1.839	.7	.397
5	1.800	1.222	1.554	33.6	.464	1.770	1.219	1.608	1.1	.373	2.101	1.282	1.825	30.1	.454	2.067	1.281	1.841	.9	.412
6	1.802	1.211	1.550	32.8	.469	1.786	1.210	1.609	.1	.388	2.101	1.273	1.823	29.4	.455	2.084	1.272	1.841	-.2	.425
7	1.809	1.202	1.545	33.3	.480	1.796	1.201	1.612	-.9	.396	2.102	1.260	1.819	28.6	.460	2.081	1.263	1.842	-2.1	.422
8	1.810	1.196	1.538	35.1	.488	1.795	1.197	1.614	-.8	.392	2.100	1.252	1.813	29.7	.463	2.075	1.257	1.841	-3.8	.418
9	1.807	1.194	1.535	36.6	.489	1.792	1.193	1.615	-1.0	.389	2.098	1.251	1.812	30.9	.463	2.071	1.261	1.840	-3.7	.415
10	1.807	1.192	1.526	38.4	.498	1.796	1.195	1.616	.2	.391	2.095	1.250	1.808	33.2	.464	2.081	1.254	1.839	-2.5	.424
11	1.803	1.195	1.522	40.1	.498	1.800	1.197	1.617	2.3	.394	2.093	1.254	1.807	36.0	.463	2.084	1.252	1.838	-1.5	.428
12	1.808	1.201	1.519	42.5	.505	1.790	1.202	1.618	3.5	.384	2.093	1.261	1.806	37.3	.465	2.084	1.254	1.838	-.6	.428
Exhaust-nozzle setting, 30; bleed closed; $w\sqrt{\theta}/\delta$, 40.48 lb/sec																				
Outer wall			1.567					1.618					1.852					1.838		
2	1.778	1.243	1.566	43.6	0.431	1.716	1.237	1.619	0.2	0.290	2.062	1.300	1.851	37.5	0.396	2.000	1.298	1.873	-3.6	0.309
3	1.791	1.242	1.564	39.8	.445	1.740	1.235	1.620	1.9	.321	2.087	1.301	1.850	34.4	.420	2.036	1.297	1.874	-.2	.346
4	1.804	1.236	1.563	36.9	.458	1.764	1.231	1.621	1.8	.350	2.104	1.296	1.849	32.4	.435	2.074	1.297	1.875	1.5	.383
5	1.804	1.228	1.559	36.0	.461	1.770	1.225	1.622	1.6	.356	2.118	1.290	1.847	32.0	.447	2.087	1.291	1.876	1.2	.394
6	1.807	1.219	1.556	35.0	.468	1.783	1.222	1.624	.9	.367	2.116	1.282	1.846	31.4	.447	2.101	1.287	1.876	.2	.406
7	1.807	1.206	1.549	35.1	.476	1.795	1.207	1.629	-.2	.376	2.114	1.267	1.842	30.8	.449	2.102	1.273	1.876	-1.6	.407
8	1.807	1.198	1.542	36.6	.483	1.795	1.199	1.631	-.9	.373	2.114	1.260	1.839	32.0	.452	2.098	1.262	1.876	-2.7	.403
9	1.802	1.196	1.538	37.8	.484	1.798	1.199	1.630	-1.1	.375	2.111	1.258	1.837	32.4	.451	2.092	1.261	1.874	-3.3	.400
10	1.801	1.195	1.532	39.4	.495	1.802	1.196	1.629	.2	.382	2.114	1.256	1.834	34.9	.457	2.101	1.258	1.873	-2.6	.408
11	1.806	1.196	1.529	40.7	.494	1.803	1.199	1.628	2.2	.384	2.105	1.260	1.831	37.2	.452	2.101	1.257	1.872	-1.4	.410
12	1.804	1.200	1.527	43.0	.505	1.795	1.203	1.627	3.3	.378	2.112	1.264	1.829	39.0	.459	2.102	1.259	1.871	-1.0	.412
Exhaust-nozzle setting, 100; bleed closed; $w\sqrt{\theta}/\delta$, 40.30 lb/sec																				
Outer wall			1.568					1.625					1.861					1.886		
2	1.782	1.244	1.567	44.2	0.433	1.730	1.240	1.628	0.2	0.297	2.080	1.303	1.860	38.3	0.404	2.021	1.301	1.888	-3.2	0.314
3	1.799	1.243	1.566	40.4	.450	1.744	1.238	1.629	2.1	.314	2.108	1.303	1.859	35.2	.428	2.056	1.302	1.889	.5	.350
4	1.811	1.237	1.564	37.8	.463	1.768	1.235	1.632	2.3	.341	2.121	1.301	1.858	33.4	.439	2.086	1.300	1.890	1.8	.378
5	1.816	1.232	1.562	36.9	.470	1.769	1.229	1.633	2.0	.340	2.132	1.293	1.857	32.9	.449	2.089	1.295	1.890	1.4	.381
6	1.818	1.222	1.559	36.0	.475	1.781	1.224	1.635	1.3	.352	2.129	1.287	1.856	32.3	.448	2.104	1.291	1.891	.4	.394
7	1.816	1.205	1.553	35.9	.478	1.797	1.209	1.637	0	.367	2.119	1.270	1.853	31.5	.443	2.116	1.276	1.891	-1.3	.404
8	1.811	1.198	1.547	37.0	.481	1.797	1.201	1.638	-1.0	.366	2.122	1.259	1.849	32.3	.449	2.109	1.266	1.891	-2.6	.428
9	1.811	1.194	1.543	37.4	.484	1.799	1.201	1.638	-.8	.369	2.124	1.257	1.847	32.8	.452	2.110	1.266	1.890	-2.5	.400
10	1.816	1.198	1.538	39.5	.493	1.801	1.200	1.637	.2	.372	2.127	1.260	1.845	35.4	.456	2.112	1.252	1.889	-2.5	.403
11	1.819	1.198	1.537	41.0	.498	1.808	1.201	1.637	2.1	.377	2.129	1.261	1.844	37.7	.458	2.110	1.261	1.887	-1.8	.403
12	1.824	1.202	1.532	43.3	.505	1.790	1.201	1.637	3.5	.380	2.129	1.263	1.843	39.3	.459	2.108	1.258	1.886	-1.5	.402

Negative angles signify turning past axial direction.

[redacted]

TABLE II. - Continued. RADIAL DISTRIBUTION OF PERFORMANCE DATA FROM FIVE-STAGE TRANSONIC COMPRESSOR

(b) Continued. Series 2.

2. Speed, 80-percent design.

Radial position	Station 7 P_7/P_2	T_7/T_2	p_7/P_2	β, deg	M	Station 8 P_8/P_2	T_8/T_2	p_8/P_2	β, deg	M	Station 9 P_9/P_2	T_9/T_2	p_9/P_2	β, deg	M	Station 10 P_{10}/P_2	T_{10}/T_2	p_{10}/P_2	β, deg	M
Exhaust-nozzle setting, 0; bleed open; $w\sqrt{\theta}/\delta$, 52.12 lb/sec																				
Outer wall			1.778					1.813					2.159					2.180		
2	2.028	1.299	1.775	40.4	0.442	1.985	1.285	1.821	-0.9	0.353	2.481	1.369	2.159	37.6	0.451	2.391	1.365	2.186	-3.9	0.361
3	2.065	1.299	1.772	37.6	.485	2.017	1.283	1.824	2.1	.382	2.521	1.367	2.158	34.0	.477	2.490	1.365	2.190	-.5	.432
4	2.106	1.284	1.769	33.9	.506	2.068	1.282	1.829	2.4	.423	2.560	1.365	2.157	31.8	.501	2.498	1.365	2.193	.9	.436
5	2.115	1.274	1.764	31.8	.517	2.079	1.274	1.832	1.1	.429	2.577	1.353	2.156	31.2	.512	2.521	1.355	2.197	.8	.448
6	2.119	1.263	1.757	31.4	.526	2.097	1.267	1.837	0	.440	2.575	1.342	2.155	30.4	.510	2.551	1.350	2.199	-.7	.465
7	2.118	1.254	1.745	33.0	.533	2.097	1.258	1.843	-1.2	.434	2.566	1.333	2.152	30.3	.509	2.543	1.339	2.202	-2.3	.459
8	2.112	1.252	1.733	35.7	.540	2.089	1.252	1.846	-.9	.424	2.550	1.330	2.140	31.5	.507	2.531	1.331	2.201	-2.9	.452
9	2.104	1.251	1.725	36.8	.541	2.086	1.252	1.847	-1.1	.421	2.548	1.330	2.129	32.7	.514	2.523	1.332	2.199	-3.4	.448
10	2.112	1.253	1.716	38.8	.554	2.089	1.252	1.847	.2	.424	2.552	1.329	2.084	35.0	.548	2.531	1.328	2.196	-2.7	.453
11	2.114	1.252	1.712	40.8	.558	2.096	1.255	1.847	2.3	.429	2.563	1.336	2.059	37.7	.565	2.536	1.328	2.197	-2.0	.458
12	2.116	1.258	1.708	43.1	.563	2.081	1.259	1.847	3.3	.417	2.556	1.339	2.045	39.1	.574	2.536	1.328	2.196	-1.0	.458
Exhaust-nozzle setting, 120; bleed closed; $w\sqrt{\theta}/\delta$, 50.30 lb/sec																				
Outer wall			1.795					1.862					2.221					2.270		
2	2.093	1.300	1.778	42.7	0.477	2.011	1.296	1.867	0	0.329	2.560	1.383	2.113	40.3	0.458	2.455	1.382	2.287	-3.0	0.334
3	2.114	1.301	1.775	38.9	.494	2.048	1.294	1.868	2.4	.363	2.585	1.384	2.102	36.9	.475	2.499	1.378	2.275	1.5	.389
4	2.126	1.291	1.768	35.5	.505	2.060	1.288	1.890	1.6	.392	2.618	1.378	2.105	35.1	.497	2.536	1.376	2.273	2.5	.397
5	2.134	1.282	1.771	34.1	.516	2.080	1.283	1.875	1.1	.400	2.631	1.370	2.109	34.5	.507	2.559	1.374	2.277	1.7	.410
6	2.141	1.274	1.774	33.7	.525	2.111	1.272	1.877	-.2	.415	2.631	1.361	2.112	33.2	.510	2.587	1.365	2.285	.2	.429
7	2.136	1.261	1.763	34.7	.531	2.112	1.263	1.879	-1.0	.413	2.611	1.344	2.149	32.3	.504	2.591	1.350	2.280	-2.0	.432
8	2.122	1.258	1.749	37.6	.531	2.109	1.252	1.880	-1.0	.408	2.593	1.339	2.130	33.9	.501	2.584	1.343	2.279	-2.5	.428
9	2.118	1.254	1.748	38.4	.534	2.105	1.254	1.883	-1.1	.403	2.590	1.335	2.131	34.5	.502	2.577	1.343	2.278	-3.0	.423
10	2.125	1.258	1.757	39.8	.547	2.108	1.260	1.886	.3	.404	2.594	1.341	2.129	36.7	.509	2.584	1.341	2.277	-2.7	.429
11	2.130	1.260	1.752	41.6	.554	2.114	1.260	1.883	2.4	.410	2.606	1.345	2.128	39.4	.518	2.583	1.341	2.277	-1.5	.429
12	2.136	1.260	1.722	44.7	.566	2.115	1.264	1.884	3.3	.411	2.612	1.348	2.123	40.9	.522	2.585	1.339	2.277	-.4	.430
Exhaust-nozzle setting, 180; bleed closed; $w\sqrt{\theta}/\delta$, 50.07 lb/sec																				
Outer wall			1.801					1.877					2.248					2.306		
2	2.116	1.310	1.797	44.6	0.489	2.031	1.303	1.880	0.1	0.335	2.564	1.395	2.254	41.8	0.446	2.481	1.388	2.307	-3.1	0.384
3	2.127	1.306	1.795	40.4	.499	2.057	1.296	1.881	2.0	.360	2.318	1.391	2.251	38.5	.469	2.533	1.384	2.309	1.8	.387
4	2.143	1.301	1.792	36.5	.512	2.090	1.294	1.883	1.8	.389	2.569	1.384	2.249	36.5	.483	2.578	1.385	2.310	2.9	.400
5	2.141	1.290	1.787	34.6	.515	2.093	1.290	1.886	1.2	.390	2.546	1.376	2.246	35.1	.490	2.599	1.378	2.311	1.9	.414
6	2.145	1.277	1.781	34.8	.521	2.105	1.277	1.887	.4	.398	2.549	1.369	2.242	34.1	.494	2.605	1.370	2.312	.6	.415
7	2.142	1.266	1.770	36.1	.529	2.121	1.265	1.892	-.5	.408	2.532	1.351	2.233	33.4	.490	2.615	1.364	2.314	-1.5	.425
8	2.134	1.262	1.758	38.5	.534	2.119	1.259	1.895	-.9	.404	2.619	1.343	2.225	35.1	.489	2.611	1.343	2.313	-2.5	.420
9	2.125	1.259	1.752	39.2	.535	2.118	1.260	1.898	-.8	.400	2.611	1.341	2.219	35.5	.488	2.602	1.344	2.315	-2.9	.414
10	2.131	1.258	1.742	40.7	.544	2.124	1.260	1.897	-.7	.406	2.606	1.341	2.215	37.9	.490	2.609	1.343	2.312	-2.5	.420
11	2.138	1.260	1.759	41.9	.551	2.128	1.261	1.897	2.5	.408	2.622	1.348	2.210	40.1	.501	2.607	1.342	2.311	-1.4	.419
12	2.158	1.264	1.755	45.3	.568	2.126	1.270	1.895	3.4	.408	2.636	1.350	2.208	42.1	.509	2.609	1.346	2.310	-.4	.421
Exhaust-nozzle setting, 250; bleed closed; $w\sqrt{\theta}/\delta$, 48.71 lb/sec																				
Outer wall			1.817					1.895					2.267					2.339		
2	2.116	1.315	1.814	45.8	0.476	2.044	1.312	1.900	0.7	0.324	2.592	1.407	2.266	44.8	0.443	2.621	1.400	2.345	-3.4	0.323
3	2.140	1.313	1.812	42.2	.485	2.058	1.306	1.902	2.9	.337	2.626	1.401	2.266	42.0	.465	2.667	1.396	2.348	1.9	.351
4	2.142	1.306	1.808	39.1	.502	2.086	1.303	1.905	2.4	.363	2.651	1.398	2.265	39.3	.481	2.603	1.397	2.351	2.5	.385
5	2.151	1.296	1.804	37.6	.508	2.087	1.295	1.907	1.9	.362	2.659	1.387	2.265	37.6	.485	2.622	1.387	2.350	2.4	.399
6	2.154	1.281	1.797	36.9	.516	2.098	1.284	1.908	1.0	.371	2.659	1.376	2.263	36.4	.486	2.636	1.378	2.351	1.0	.408
7	2.153	1.269	1.787	37.4	.524	2.117	1.274	1.911	0	.386	2.657	1.367	2.260	35.6	.487	2.636	1.364	2.350	-1.4	.409
8	2.149	1.262	1.774	39.0	.531	2.124	1.263	1.912	-.8	.391	2.646	1.346	2.253	36.1	.486	2.627	1.351	2.349	-2.7	.403
9	2.136	1.256	1.767	39.8	.528	2.124	1.257	1.913	-.8	.390	2.634	1.343	2.249	36.2	.461	2.624	1.346	2.349	-3.0	.402
10	2.146	1.260	1.755	41.4	.544	2.129	1.263	1.913	.7	.393	2.640	1.346	2.242	38.3	.489	2.624	1.347	2.348	-2.6	.402
11	2.151	1.262	1.750	43.0	.552	2.136	1.265	1.915	2.7	.398	2.655	1.349	2.238	41.0	.501	2.625	1.347	2.348	-1.4	.403
12	2.169	1.268	1.743	46.2	.568	2.124	1.269	1.917	3.4	.386	2.665	1.354	2.235	43.2	.506	2.633	1.346	2.346	-.6	.406

Negative angles signify turning past axial direction.

[redacted]

TABLE II. - Continued. RADIAL DISTRIBUTION OF PERFORMANCE DATA FROM FIVE-STAGE TRANSONIC COMPRESSOR

(b) Continued. Series 2.

3. Speed, 90-percent design.

Radial position	Station 7					Station 8					Station 9					Station 10				
	P_7/P_2	T_7/T_2	p_7/P_2	β, deg	M	P_8/P_2	T_8/T_2	p_8/P_2	β, deg	M	P_9/P_2	T_9/T_2	p_9/P_2	β, deg	M	P_{10}/P_2	T_{10}/T_2	p_{10}/P_2	β, deg	M
Exhaust-nozzle setting, 0; bleed open; $w\sqrt{\theta}/\delta$, 64.22 lb/sec																				
Outer wall			1.987					2.082					2.593					2.852		
2	2.355	1.369	1.985	39.2	0.488	2.293	1.359	2.065	-0.1	0.390	3.080	1.470	2.584	39.0	0.502	2.832	1.469	2.858	-1.6	0.378
3	2.378	1.362	1.982	37.4	.517	2.338	1.351	2.067	3.3	.424	3.138	1.467	2.591	36.0	.530	3.010	1.461	2.861	2.8	.424
4	2.443	1.354	1.978	35.9	.557	2.408	1.350	2.070	3.1	.470	3.155	1.464	2.588	33.7	.540	3.078	1.460	2.864	2.9	.460
5	2.473	1.341	1.974	32.1	.577	2.428	1.344	2.073	1.6	.481	3.173	1.452	2.584	32.1	.550	3.098	1.452	2.867	1.7	.468
6	2.476	1.330	1.968	31.0	.583	2.455	1.330	2.076	.1	.498	3.164	1.440	2.579	31.3	.548	3.125	1.439	2.871	.7	.480
7	2.484	1.319	1.958	32.3	.584	2.462	1.317	2.083	-1.3	.498	3.154	1.425	2.568	30.3	.551	3.128	1.425	2.873	-1.3	.480
8	2.472	1.315	1.942	34.7	.598	2.464	1.313	2.087	-.7	.493	3.148	1.418	2.555	32.4	.556	3.121	1.419	2.872	-1.9	.477
9	2.476	1.315	1.933	36.0	.607	2.453	1.313	2.090	-.8	.484	3.144	1.416	2.551	33.9	.558	3.116	1.417	2.870	-2.3	.478
10	2.480	1.318	1.917	38.2	.618	2.454	1.312	2.092	1.0	.483	3.133	1.422	2.543	36.4	.565	3.114	1.418	2.867	-1.7	.478
11	2.485	1.316	1.910	40.5	.626	2.455	1.313	2.095	2.6	.483	3.131	1.422	2.539	39.0	.556	3.112	1.415	2.865	-.6	.476
12	2.489	1.327	1.894	43.6	.638	2.428	1.321	2.094	3.4	.485	3.135	1.433	2.537	41.0	.559	2.843	1.417	2.865	.6	.508
Exhaust-nozzle setting, 90; bleed closed; $w\sqrt{\theta}/\delta$, 62.14 lb/sec																				
Outer wall			2.039					2.137					2.698					2.792		
2	2.446	1.373	2.036	42.0	0.520	2.343	1.367	2.142	1.9	0.381	3.182	1.485	2.697	43.7	0.483	3.057	1.480	2.794	-2.8	0.362
3	2.465	1.371	2.034	37.8	.532	2.384	1.360	2.148	2.7	.385	3.215	1.482	2.696	40.9	.509	3.086	1.476	2.795	1.9	.385
4	2.508	1.365	2.030	34.9	.558	2.455	1.357	2.145	2.1	.446	3.251	1.476	2.695	38.4	.526	3.167	1.474	2.798	3.9	.498
5	2.535	1.350	2.026	33.4	.575	2.487	1.349	2.147	1.0	.461	3.280	1.462	2.693	36.2	.531	3.184	1.467	2.798	2.5	.454
6	2.541	1.339	2.019	32.9	.584	2.483	1.336	2.151	.1	.459	3.263	1.455	2.690	34.8	.533	3.202	1.457	2.799	.7	.463
7	2.524	1.323	2.004	34.4	.584	2.491	1.323	2.157	-1.0	.458	3.247	1.431	2.682	34.1	.530	3.214	1.440	2.801	-2.1	.448
8	2.508	1.319	1.986	36.6	.589	2.474	1.319	2.162	-.6	.444	3.234	1.427	2.671	35.4	.531	3.202	1.427	2.802	-2.9	.442
9	2.484	1.313	1.975	38.4	.588	2.473	1.316	2.163	-.3	.443	3.223	1.425	2.664	36.6	.530	3.197	1.426	2.801	-2.6	.440
10	2.489	1.316	1.957	41.1	.602	2.476	1.320	2.163	.9	.445	3.215	1.428	2.651	39.7	.533	3.188	1.426	2.799	-1.7	.442
11	2.509	1.320	1.949	42.8	.612	2.486	1.324	2.162	1.7	.452	3.231	1.428	2.644	42.3	.544	3.188	1.428	2.798	-.9	.442
12	2.525	1.328	1.940	45.3	.626	2.481	1.327	2.161	2.9	.449	3.240	1.433	2.639	44.0	.561	3.186	1.425	2.794	-.3	.443
Exhaust-nozzle setting, 180; bleed closed; $w\sqrt{\theta}/\delta$, 62.10 lb/sec																				
Outer wall			2.065					2.166					2.731					2.834		
2	2.481	1.377	2.062	43.1	0.522	2.348	1.370	2.163	-0.3	0.365	3.231	1.492	2.730	44.5	0.497	3.102	1.489	2.836	-4.0	0.361
3	2.501	1.376	2.059	39.4	.535	2.402	1.364	2.166	1.4	.387	3.242	1.487	2.729	41.8	.503	3.127	1.482	2.837	1.1	.376
4	2.539	1.363	2.055	35.6	.559	2.463	1.360	2.170	1.6	.430	3.284	1.481	2.728	39.3	.522	3.197	1.480	2.839	2.6	.416
5	2.554	1.348	2.049	34.4	.571	2.482	1.351	2.173	.6	.441	3.302	1.471	2.727	37.4	.531	3.214	1.473	2.840	2.8	.424
6	2.557	1.341	2.041	34.6	.578	2.503	1.342	2.176	0	.452	3.299	1.460	2.725	36.0	.530	3.236	1.463	2.841	1.9	.436
7	2.542	1.328	2.027	36.2	.579	2.505	1.328	2.180	-.9	.451	3.284	1.440	2.720	35.3	.526	3.246	1.442	2.842	.5	.441
8	2.530	1.324	2.008	38.6	.586	2.498	1.322	2.182	-.6	.444	3.266	1.436	2.719	36.7	.525	3.238	1.433	2.841	-.4	.437
9	2.513	1.321	1.998	39.7	.584	2.481	1.320	2.184	0	.431	3.249	1.432	2.706	37.8	.518	3.223	1.430	2.839	-.7	.430
10	2.525	1.322	1.979	41.8	.602	2.488	1.322	2.186	1.1	.434	3.261	1.435	2.694	40.5	.530	3.219	1.430	2.837	-.8	.429
11	2.529	1.324	1.970	43.3	.609	2.499	1.327	2.187	1.8	.441	3.282	1.438	2.685	43.5	.544	3.233	1.434	2.834	-.8	.439
12	2.556	1.330	1.954	46.2	.632	2.493	1.332	2.189	2.8	.436	3.306	1.441	2.678	45.5	.558	3.234	1.436	2.833	-.8	.440
Exhaust-nozzle setting, 240; bleed closed; $w\sqrt{\theta}/\delta$, 60.84 lb/sec																				
Outer wall			2.085					2.179					2.745					2.871		
2	2.469	1.377	2.070	43.9	0.499	2.400	1.373	2.182	1.8	0.371	3.189	1.501	2.726	46.5	0.470	3.106	1.490	2.873	-0.3	0.338
3	2.486	1.375	2.069	40.8	.510	2.444	1.367	2.185	2.5	.403	3.222	1.496	2.716	44.4	.487	3.170	1.486	2.873	2.2	.377
4	2.527	1.365	2.072	37.2	.535	2.475	1.361	2.190	1.3	.422	3.268	1.490	2.721	41.7	.509	3.214	1.480	2.871	1.6	.402
5	2.536	1.348	2.068	35.8	.542	2.485	1.357	2.192	1.0	.428	3.288	1.475	2.721	38.8	.520	3.238	1.474	2.876	.4	.414
6	2.534	1.337	2.071	35.1	.546	2.501	1.342	2.199	.2	.435	3.291	1.463	2.719	37.7	.525	3.257	1.461	2.879	.2	.424
7	2.540	1.327	2.084	35.8	.557	2.514	1.321	2.204	-.9	.440	3.282	1.444	2.715	36.4	.516	3.269	1.449	2.879	-1.9	.425
8	2.528	1.319	2.012	39.2	.559	2.504	1.319	2.202	-.8	.430	3.246	1.431	2.711	38.2	.515	2.262	1.430	2.879	-2.7	.422
9	2.518	1.321	2.059	40.0	.560	2.501	1.318	2.210	-.6	.427	3.244	1.431	2.702	39.1	.518	3.243	1.427	2.882	-3.0	.417
10	2.530	1.318	2.022	42.1	.573	2.507	1.315	2.205	.9	.430	3.263	1.431	2.687	41.2	.532	3.245	1.428	2.868	-1.8	.420
11	2.537	1.322	2.023	44.0	.579	2.513	1.317	2.209	2.7	.434	3.272	1.435	2.682	43.6	.540	3.245	1.428	2.866	.2	.420
12	2.549	1.331	2.019	46.4	.598	2.511	1.322	2.211	4.7	.433	3.300	1.442	2.689	45.0	.554	3.258	1.429	2.875	1.4	.427

Negative angles signify turning past axial direction.

TABLE II. - Continued. RADIAL DISTRIBUTION OF PERFORMANCE DATA FROM FIVE-STAGE TRANSONIC COMPRESSOR

(b) Concluded. Series 2.

4. Speed, 100-percent design.

Radial position	Station 7					Station 8					Station 9					Station 10				
	P_7/P_2	T_7/T_2	p_7/P_2	β, deg	M	P_8/P_2	T_8/T_2	p_8/P_2	β, deg	M	P_9/P_2	T_9/T_2	p_9/P_2	β, deg	M	P_{10}/P_2	T_{10}/T_2	p_{10}/P_2	β, deg	M
Exhaust-nozzle setting, 0; bleed open; $w_A\sqrt{\theta}/\delta$, 68.86 lb/sec																				
Outer wall			2.008					2.089					2.783					2.920		
2	2.384	1.465	2.009	46.2	0.501	2.330	1.425	2.090	2.9	0.398	3.272	1.614	2.784	48.0	0.487	3.210	1.575	2.923	1.3	0.388
3	2.416	1.461	2.009	43.1	.521	2.381	1.421	2.091	2.3	.435	3.343	1.606	2.784	45.7	.519	3.287	1.566	2.927	3.0	.411
4	2.456	1.437	2.009	38.4	.543	2.424	1.410	2.093	.7	.465	3.393	1.589	2.784	41.7	.540	3.348	1.561	2.928	1.7	.442
5	2.519	1.424	2.009	34.7	.579	2.447	1.411	2.096	.2	.476	3.440	1.576	2.783	38.0	.560	3.373	1.554	2.928	-.1	.454
6	2.554	1.402	2.008	33.4	.598	2.501	1.388	2.099	.1	.507	3.470	1.566	2.782	36.4	.572	3.420	1.528	2.928	-.1	.477
7	2.606	1.386	2.003	33.6	.625	2.550	1.374	2.109	-.2	.528	3.492	[illegible]	2.776	34.5	.582	3.464	1.508	2.928	-1.0	.496
8	2.630	1.379	1.996	34.7	.641	2.590	1.357	2.118	-.1	.544	3.486	1.506	2.768	35.4	.576	3.464	1.491	2.927	-1.9	.497
9	2.643	1.375	1.992	35.6	.650	2.600	1.355	2.123	-.3	.546	3.481	1.503	2.763	36.0	.577	3.461	1.489	2.928	-2.6	.496
10	2.651	1.377	1.986	35.7	.657	2.631	1.358	2.128	.4	.559	3.479	1.506	2.756	37.8	.587	3.478	1.490	2.926	-2.0	.502
11	2.653	1.377	1.983	37.4	.659	2.631	1.360	2.130	1.6	.558	3.492	1.504	2.752	40.2	.584	3.459	1.484	2.926	-.6	.496
12	2.663	1.383	1.980	40.8	.665	2.591	1.360	2.132	4.4	.536	3.491	1.510	2.751	42.3	.594	3.468	1.484	2.926	.8	.500
Exhaust-nozzle setting, 240; bleed closed; $w_A\sqrt{\theta}/\delta$, 68.72 lb/sec																				
Outer wall			2.226					2.368					3.137					3.364		
2	2.722	1.484	2.226	49.5	0.544	2.602	1.452	2.370	2.0	0.388	3.741	1.649	3.132	54.2	0.511	3.687	1.609	3.358	5.0	0.354
3	2.765	1.475	2.220	44.1	.569	2.651	1.447	2.371	1.9	.389	3.762	1.646	3.128	50.3	.521	3.731	1.602	3.356	3.7	.392
4	2.765	1.466	2.214	39.8	.573	2.686	1.436	2.373	.1	.425	3.788	1.632	3.124	46.4	.532	3.775	1.593	3.356	2.8	.413
5	2.774	1.437	2.209	38.3	.561	2.688	1.428	2.374	-.1	.426	3.830	1.612	3.119	43.5	.550	3.774	1.584	3.358	.6	.414
6	2.788	1.420	2.200	36.9	.593	2.716	1.417	2.378	.1	.442	3.852	1.596	3.114	41.1	.561	3.799	1.573	3.354	.6	.428
7	2.822	1.398	2.186	36.1	.618	2.775	1.393	2.379	-.6	.474	3.830	1.557	3.100	38.7	.559	3.822	1.546	3.351	-1.4	.438
8	2.807	1.384	2.172	37.9	.617	2.772	1.376	2.383	-1.4	.470	3.802	1.552	3.085	39.4	.555	3.806	1.526	3.344	-2.7	.434
9	2.806	1.385	2.165	38.7	.622	2.777	1.370	2.384	-1.5	.473	3.800	1.526	3.080	40.8	.557	3.806	1.517	3.338	-2.9	.437
10	2.828	1.380	2.158	40.7	.637	2.772	1.374	2.386	0	.469	3.843	1.526	3.070	42.7	.576	3.802	1.517	3.331	-2.0	.440
11	2.853	1.385	2.151	42.9	.641	2.761	1.371	2.386	1.8	.462	3.854	1.526	3.066	45.6	.582	3.791	1.511	3.326	-.2	.437
12	2.854	1.396	2.147	47.0	.643	2.738	1.374	2.387	4.0	.448	3.889	1.536	3.063	47.8	.592	3.809	1.508	3.323	.5	.447
Exhaust-nozzle setting, 210; bleed closed; $w_A\sqrt{\theta}/\delta$, 68.70 lb/sec																				
Outer wall			2.169					2.304					3.079					3.285		
2	2.663	1.461	2.162	49.4	0.555	2.550	1.448	2.309	2.3	0.380	3.664	1.626	3.074	52.3	0.508	3.561	1.603	3.285	2.8	0.342
3	2.686	1.456	2.161	44.9	.567	2.577	1.438	2.311	2.2	.398	3.685	1.623	3.071	48.9	.518	3.638	1.590	3.285	3.2	.386
4	2.703	1.446	2.159	39.8	.576	2.633	1.430	2.315	.4	.433	3.731	1.611	3.066	45.7	.537	3.661	1.586	3.284	1.6	.406
5	2.706	1.423	2.157	37.3	.580	2.644	1.428	2.319	0	.438	3.771	1.582	3.063	42.4	.554	3.707	1.577	3.284	0	.420
6	2.748	1.408	2.153	36.0	.602	2.677	1.410	2.324	.1	.455	3.806	1.577	3.058	40.3	.548	3.731	1.561	3.283	-.4	.438
7	2.763	1.385	2.144	35.4	.614	2.741	1.384	2.332	-.7	.487	3.756	1.538	3.046	38.2	.556	3.758	1.536	3.282	-1.1	.445
8	2.761	1.381	2.133	36.5	.619	2.743	1.374	2.339	-1.6	.484	3.730	1.526	3.033	38.9	.553	3.757	1.520	3.279	-3.0	.446
9	2.769	1.372	2.127	37.1	.628	2.746	1.370	2.342	-1.4	.483	3.738	1.518	3.027	39.8	.558	3.756	1.514	3.276	-3.0	.447
10	2.789	1.374	2.120	39.5	.639	2.734	1.369	2.345	0	.474	3.771	1.517	3.017	42.1	.574	3.737	1.511	3.273	-1.9	.440
11	2.794	1.380	2.117	41.8	.643	2.737	1.371	2.347	1.6	.476	3.768	1.519	3.013	44.9	.582	3.744	1.509	3.272	-.7	.444
12	2.784	1.376	2.114	46.1	.640	2.706	1.374	2.349	3.7	.456	3.792	1.519	3.011	48.6	.586	3.752	1.506	3.268	.2	.449
Exhaust-nozzle setting, 180; bleed closed; $w_A\sqrt{\theta}/\delta$, 68.73 lb/sec																				
Outer wall			2.124					2.253					3.017					3.206		
2	2.614	1.479	2.123	49.0	0.554	2.509	1.455	2.261	2.4	0.389	3.588	1.643	3.014	52.6	0.506	3.525	1.607	3.212	2.3	0.368
3	2.643	1.489	2.122	44.7	.570	2.537	1.446	2.265	2.3	.408	3.624	1.638	3.012	49.1	.522	3.606	1.598	3.216	2.5	.408
4	2.658	1.460	2.120	39.1	.578	2.598	1.432	2.271	.4	.443	3.685	1.626	3.010	45.5	.546	3.650	1.587	3.219	-.5	.428
5	2.685	1.434	2.119	37.0	.593	2.611	1.424	2.276	.6	.446	3.742	1.603	3.007	41.9	.569	3.653	1.574	3.222	-.2	.428
6	2.699	1.414	2.118	35.7	.601	2.654	1.412	2.282	-.1	.476	3.739	1.590	3.004	40.0	.569	3.700	1.560	3.224	-.5	.449
7	2.738	1.384	2.111	34.9	.622	2.705	1.388	2.292	-.6	.493	3.724	1.562	2.995	38.0	.567	3.714	1.536	3.225	-1.9	.454
8	2.746	1.384	2.105	35.8	.629	2.714	1.367	2.300	-1.0	.495	3.699	1.527	2.985	38.7	.563	3.701	1.511	3.224	-3.6	.449
9	2.746	1.377	2.101	36.3	.631	2.710	1.367	2.304	-1.7	.488	3.703	1.520	2.979	39.3	.567	3.694	1.509	3.222	-3.6	.447
10	2.770	1.380	2.095	38.3	.645	2.712	1.370	2.308	-.2	.487	3.739	1.522	2.970	41.6	.584	3.689	1.506	3.220	-2.4	.446
11	2.777	1.384	2.092	40.9	.650	2.710	1.372	2.310	1.4	.484	3.756	1.526	2.965	44.3	.585	3.697	1.510	3.218	-1.1	.450
12	2.768	1.386	2.089	44.3	.648	2.682	1.371	2.312	3.8	.486	3.782	1.528	2.962	46.6	.592	3.706	1.505	3.217	.5	.455

Negative angles signify turning past axial direction.

[redacted]

TABLE II. - Continued. RADIAL DISTRIBUTION OF PERFORMANCE DATA FROM FIVE-STAGE TRANSONIC COMPRESSOR

(c) Series 3.

1. Speed, 70-percent design.

Radial position	Station 11 P_{11}/P_2	T_{11}/T_2	p_{11}/P_2	β, deg	M	Station 12 P_{12}/P_2	T_{12}/T_2	p_{12}/P_2	β, deg	M
Exhaust-nozzle setting, 0; bleed open; $w\sqrt{\theta}/\delta$, 41.33 lb/sec										
Outer wall			2.038					2.043		
2	2.210	1.354	2.037	27.7	0.343	2.165	1.353	2.046	-4.6	0.286
3	2.260	1.353	2.038	22.4	.388	2.212	1.354	2.048	.2	.355
4	2.298	1.331	2.039	20.4	.417	2.280	1.334	2.050	2.0	.377
5	2.324	1.323	2.039	19.4	.437	2.282	1.326	2.051	2.2	.393
6	2.337	1.316	2.040	17.8	.448	2.302	1.317	2.054	.3	.407
7	2.332	1.303	2.041	17.0	.441	2.304	1.310	2.056	-1.7	.407
8	2.331	1.300	2.041	18.1	.441	2.291	1.302	2.058	-1.4	.395
9	2.328	1.298	2.041	19.3	.439	2.292	1.301	2.058	0	.396
10	2.326	1.300	2.040	20.3	.437	2.303	1.302	2.058	2.0	.404
11	2.321	1.302	2.040	23.4	.433	2.291	1.304	2.059	3.6	.394
12	2.314	1.304	2.040	26.6	.429	2.297	1.306	2.058	4.3	.385
Exhaust-nozzle setting, 30; bleed closed; $w\sqrt{\theta}/\delta$, 40.22 lb/sec										
Outer wall			2.102					2.123		
2	2.322	1.350	2.103	28.9	0.379	2.240	1.353	2.122	-1.5	0.279
3	2.322	1.347	2.103	26.6	.379	2.273	1.349	2.121	-.5	.316
4	2.342	1.345	2.103	24.9	.396	2.314	1.343	2.121	.3	.355
5	2.368	1.338	2.104	23.2	.415	2.338	1.339	2.121	.3	.375
6	2.381	1.332	2.104	21.8	.425	2.347	1.331	2.122	-.1	.383
7	2.381	1.319	2.104	20.6	.426	2.350	1.320	2.123	-2.2	.384
8	2.370	1.312	2.103	21.1	.418	2.348	1.312	2.124	-2.6	.380
9	2.369	1.310	2.102	21.2	.417	2.347	1.310	2.123	-1.8	.381
10	2.372	1.310	2.100	23.7	.421	2.353	1.310	2.122	1.6	.387
11	2.371	1.314	2.099	27.4	.421	2.345	1.311	2.121	3.2	.382
12	2.366	1.318	2.099	29.5	.418	2.334	1.311	2.120	4.5	.374
Exhaust-nozzle setting, 0; bleed half open; $w\sqrt{\theta}/\delta$, 41.12 lb/sec										
Outer wall			2.061					2.094		
2	2.305	1.342	2.063	25.9	0.384	2.219	1.340	2.095	-1.4	0.268
3	2.306	1.340	2.064	26.0	.383	2.231	1.341	2.095	-.8	.322
4	2.327	1.337	2.064	23.8	.401	2.295	1.338	2.096	-.6	.363
5	2.347	1.328	2.065	21.7	.416	2.321	1.334	2.096	-.4	.385
6	2.368	1.323	2.065	19.5	.431	2.331	1.326	2.096	-.7	.393
7	2.368	1.313	2.064	18.7	.432	2.340	1.318	2.096	-2.8	.400
8	2.362	1.307	2.063	20.1	.428	2.329	1.307	2.094	-3.5	.393
9	2.360	1.306	2.063	21.3	.426	2.338	1.304	2.093	-1.8	.389
10	2.358	1.304	2.063	22.7	.425	2.339	1.302	2.091	2.0	.403
11	2.356	1.307	2.063	25.3	.425	2.330	1.307	2.090	4.0	.398
12	2.354	1.310	2.063	27.6	.422	2.316	1.309	2.089	5.6	.388

2. Speed, 80-percent design.

Radial position	Station 11 P_{11}/P_2	T_{12}/T_2	p_{11}/P_2	β, deg	M	Station 12 P_{12}/P_2	T_{12}/T_2	p_{12}/P_2	β, deg	M
Exhaust-nozzle setting, 0; bleed open; $w\sqrt{\theta}/\delta$, 52.02 lb/sec										
Outer wall			2.552					2.587		
2	2.816	1.435	2.552	31.4	0.379	2.759	1.437	2.587	-3.5	0.304
3	2.882	1.433	2.551	28.9	.422	2.814	1.435	2.587	-.3	.349
4	2.923	1.429	2.550	24.7	.446	2.873	1.431	2.588	2.3	.390
5	2.961	1.422	2.550	22.8	.468	2.904	1.426	2.588	2.1	.410
6	2.980	1.412	2.548	20.9	.479	2.917	1.416	2.588	.6	.417
7	2.967	1.397	2.548	20.7	.473	2.920	1.405	2.589	-1.5	.419
8	2.952	1.395	2.545	22.1	.466	2.912	1.399	2.589	-.8	.414
9	2.942	1.393	2.545	23.0	.462	2.915	1.397	2.589	-.1	.416
10	2.941	1.398	2.543	24.7	.461	2.922	1.399	2.589	2.4	.420
11	2.938	1.401	2.542	27.6	.460	2.902	1.403	2.589	3.3	.408
12	2.858	1.405	2.541	29.9	.459	2.882	1.406	2.589	4.2	.395
Exhaust-nozzle setting, 120; bleed closed; $w\sqrt{\theta}/\delta$, 49.54 lb/sec										
Outer wall			2.650					2.707		
2	2.891	1.455	2.652	35.5	0.355	2.884	1.453	2.709	2.7	0.301
3	2.954	1.456	2.653	32.6	.396	2.930	1.453	2.710	4.2	.338
4	2.997	1.457	2.654	29.4	.422	2.985	1.449	2.712	3.9	.372
5	3.023	1.446	2.654	27.3	.438	3.001	1.446	2.714	3.4	.382
6	3.032	1.434	2.654	25.9	.441	3.015	1.436	2.717	2.6	.389
7	3.031	1.418	2.654	24.0	.441	3.021	1.422	2.720	-.1	.391
8	3.029	1.411	2.652	24.7	.436	3.020	1.414	2.722	-.4	.388
9	3.026	1.409	2.651	25.3	.440	3.015	1.413	2.722	.3	.385
10	3.044	1.411	2.648	28.1	.451	3.015	1.413	2.720	4.0	.387
11	3.042	1.414	2.647	31.7	.451	2.995	1.416	2.717	5.0	.376
12	3.045	1.418	2.647	34.6	.453	2.985	1.417	2.715	6.7	.371
Exhaust-nozzle setting, 180; bleed closed; $w\sqrt{\theta}/\delta$, 49.07 lb/sec										
Outer wall			2.692					2.758		
2	2.938	1.466	2.693	38.9	0.356	2.928	1.462	2.757	-3.1	0.295
3	2.998	1.465	2.693	34.5	.396	2.976	1.458	2.758	2.8	.332
4	3.032	1.458	2.692	31.2	.416	3.019	1.458	2.759	3.8	.362
5	3.058	1.447	2.691	28.6	.429	3.032	1.451	2.759	4.3	.370
6	3.054	1.441	2.690	26.9	.431	3.046	1.443	2.760	2.1	.379
7	3.062	1.424	2.686	25.7	.432	3.049	1.428	2.761	-.2	.380
8	3.046	1.412	2.682	25.9	.431	3.045	1.417	2.762	-.6	.377
9	3.062	1.412	2.680	26.6	.436	3.045	1.418	2.761	.2	.377
10	3.073	1.415	2.679	29.6	.446	3.044	1.419	2.761	2.8	.377
11	3.077	1.415	2.681	32.5	.449	3.037	1.419	2.761	5.3	.372
12	3.090	1.422	2.683	35.4	.455	3.026	1.424	2.760	6.6	.368
Exhaust-nozzle setting, 250; bleed closed; $w\sqrt{\theta}/\delta$, 48.28 lb/sec										
Outer wall			2.753					2.825		
2	2.981	1.488	2.752	40.0	0.340	2.972	1.487	2.826	2.4	0.269
3	3.037	1.484	2.750	38.1	.380	3.018	1.489	2.827	2.4	.307
4	3.083	1.480	2.748	34.4	.409	3.062	1.471	2.828	2.3	.340
5	3.105	1.466	2.745	30.0	.424	3.082	1.465	2.828	2.6	.350
6	3.113	1.453	2.741	28.7	.431	3.102	1.457	2.829	2.1	.366
7	3.108	1.437	2.734	27.3	.432	3.097	1.436	2.830	-.2	.361
8	3.115	1.429	2.728	27.8	.441	3.095	1.420	2.831	-.7	.360
9	3.116	1.429	2.724	29.7	.443	3.098	1.417	2.831	-.2	.361
10	3.129	1.428	2.720	31.3	.453	3.099	1.419	2.832	5.3	.361
11	3.142	1.430	2.717	34.5	.461	3.082	1.425	2.832	8.4	.360
12	3.157	1.434	2.716	37.5	.470	3.079	1.429	2.832	9.0	.348

Negative angles signify turning past axial direction.

TABLE II. - Concluded. RADIAL DISTRIBUTION OF PERFORMANCE DATA FROM FIVE-STAGE TRANSONIC COMPRESSOR

(c) Concluded. Series 3.

3. Speed, 90-percent design.

Radial position	Station 11 P_{11}/P_2	T_{11}/T_2	p_{11}/P_2	β, deg	M	Station 12 P_{12}/P_2	T_{12}/T_2	p_{12}/P_2	β, deg	M
Exhaust-nozzle setting, 0; bleed open; $w\sqrt{\theta}/\delta$, 62.81 lb/sec										
Outer wall			3.244					3.337		
2	3.590	1.559	3.243	37.6	0.385	3.567	1.581	3.336	-4.0	0.310
3	3.661	1.557	3.241	35.6	.431	3.638	1.562	3.339	2.0	.355
4	3.737	1.556	3.239	32.3	.458	3.689	1.551	3.339	1.9	.381
5	3.768	1.542	3.236	29.0	.473	3.707	1.546	3.339	.3	.390
6	3.792	1.527	3.232	27.2	.484	3.741	1.534	3.340	-.8	.407
7	3.776	1.510	3.226	26.2	.481	3.746	1.517	3.341	-1.0	.410
8	3.761	1.504	3.219	26.7	.478	3.748	1.510	3.342	-1.4	.409
9	3.765	1.505	3.215	27.5	.482	3.751	1.506	3.342	-.3	.410
10	3.771	1.508	3.210	30.0	.486	3.743	1.510	3.343	.6	.406
11	3.780	1.517	3.206	33.2	.492	3.719	1.517	3.343	3.3	.394
12	3.784	1.518	3.205	35.7	.494	3.707	1.522	3.343	4.5	.388
Exhaust-nozzle setting, 90; bleed closed; $w\sqrt{\theta}/\delta$, 61.80 lb/sec										
Outer wall			3.416					3.539		
2	3.748	1.594	3.416	40.6	0.367	3.743	1.582	3.541	-3.7	0.284
3	3.801	1.586	3.415	39.0	.395	3.788	1.580	3.541	3.8	.315
4	3.872	1.582	3.414	36.5	.429	3.858	1.577	3.541	3.1	.351
5	3.938	1.572	3.412	31.4	.457	3.874	1.571	3.542	4.0	.361
6	3.943	1.557	3.410	30.0	.462	3.898	1.562	3.542	1.8	.373
7	3.943	1.538	3.404	29.1	.464	3.915	1.541	3.541	-.2	.383
8	3.939	1.528	3.399	28.9	.465	3.910	1.527	3.537	-.6	.382
9	3.960	1.527	3.395	30.0	.475	3.917	1.527	3.535	.3	.387
10	3.975	1.527	3.391	32.9	.483	3.911	1.530	3.531	2.6	.386
11	4.001	1.529	3.390	36.7	.494	3.899	1.532	3.528	5.2	.382
12	4.017	1.539	3.389	39.4	.500	3.894	1.538	3.528	6.6	.380
Exhaust-nozzle setting, 180; bleed closed; $w\sqrt{\theta}/\delta$, 61.05 lb/sec										
Outer wall			3.469					3.598		
2	3.824	1.596	3.461	40.3	0.381	3.811	1.589	3.600	-1.5	0.287
3	3.898	1.596	3.461	39.4	.416	3.880	1.587	3.602	-.8	.317
4	3.934	1.598	3.462	36.9	.432	3.925	1.580	3.604	-1.2	.352
5	3.997	1.577	3.461	32.6	.459	3.934	1.569	3.608	-2.0	.365
6	3.992	1.562	3.460	31.1	.458	3.969	1.563	3.612	-1.8	.371
7	4.001	1.544	3.456	30.3	.463	3.977	1.544	3.617	-3.0	.371
8	3.997	1.534	3.450	29.4	.464	3.981	1.531	3.619	-4.7	.372
9	4.007	1.534	3.445	31.4	.471	3.985	1.526	3.617	-3.2	.375
10	4.024	1.531	3.440	34.0	.480	3.992	1.530	3.614	-1.8	.381
11	4.060	1.540	3.435	38.3	.496	3.975	1.533	3.609	.2	.375
12	4.070	1.544	3.432	40.5	.500	3.972	1.530	3.608	2.2	.375
Exhaust-nozzle setting, 240; bleed closed; $w\sqrt{\theta}/\delta$, 59.99 lb/sec										
Outer wall			3.536					3.691		
2	4.000	1.616	3.538	40.8	0.423	3.085	1.605	3.692	0.9	0.271
3	4.000	1.616	3.538	38.8	.424	3.920	1.605	3.693	.9	.300
4	4.011	1.615	3.535	36.5	.430	3.983	1.599	3.693	1.0	.331
5	4.061	1.599	3.531	33.1	.452	4.011	1.584	3.694	.3	.346
6	4.089	1.580	3.527	31.2	.457	4.019	1.580	3.694	0	.350
7	4.067	1.558	3.517	30.5	.457	4.048	1.564	3.694	-1.5	.365
8	4.060	1.552	3.510	30.9	.462	4.044	1.549	3.693	-2.9	.364
9	4.090	1.547	3.504	32.4	.476	4.058	1.544	3.693	-2.3	.371
10	4.110	1.548	3.498	36.0	.487	4.061	1.546	3.693	1.6	.372
11	4.132	1.552	3.493	39.7	.497	4.053	1.548	3.693	4.9	.368
12	4.128	1.559	3.490	42.0	.496	4.027	1.548	3.694	8.0	.354

4. Speed, 100-percent design.

Radial position	Station 11 P_{11}/P_2	T_{11}/T_2	p_{11}/P_2	β, deg	M	Station 12 P_{12}/P_2	T_{12}/T_2	p_{12}/P_2	β, deg	M
Exhaust-nozzle setting, 0; bleed open; $w\sqrt{\theta}/\delta$, 68.73 lb/sec										
Outer wall			3.825					4.017		
2	4.473	1.746	3.826	41.1	0.479	4.258	1.712	4.016	0.5	0.290
3	4.436	1.735	3.826	41.4	.466	4.313	1.714	4.016	1.8	.321
4	4.466	1.727	3.825	37.4	.478	4.378	1.703	4.016	1.0	.354
5	4.518	1.704	3.823	34.7	.496	4.409	1.693	4.016	.1	.368
6	4.518	1.689	3.820	32.7	.497	4.421	1.679	4.016	-.1	.373
7	4.514	1.667	3.813	29.9	.499	4.462	1.650	4.017	-2.8	.392
8	4.518	1.658	3.803	30.9	.504	4.465	1.631	4.015	-3.9	.394
9	4.565	1.638	3.796	31.5	.519	4.471	1.623	4.015	-3.4	.396
10	4.563	1.636	3.786	35.3	.525	4.456	1.629	4.016	-1.0	.390
11	4.575	1.644	3.781	39.1	.530	4.426	1.632	4.015	1.5	.377
12	4.581	1.647	3.777	41.0	.534	4.414	1.630	4.016	2.3	.371
Exhaust-nozzle setting, 240; bleed closed; $w\sqrt{\theta}/\delta$, 68.45 lb/sec										
Outer wall			4.366					4.570		
2	5.022	1.786	4.361	55.3	0.455	4.883	1.764	4.576	6.1	0.308
3	5.039	1.779	4.356	50.4	.462	4.912	1.761	4.576	6.1	.320
4	5.066	1.771	4.350	46.4	.473	4.967	1.757	4.582	6.0	.343
5	5.094	1.758	4.342	42.4	.485	4.969	1.748	4.588	4.2	.342
6	5.126	1.739	4.333	39.8	.498	4.974	1.727	4.591	2.0	.341
7	5.084	1.697	4.316	38.3	.491	5.002	1.701	4.597	2.8	.351
8	5.049	1.677	4.299	37.9	.486	5.009	1.692	4.600	1.7	.352
9	5.055	1.672	4.289	38.7	.492	5.005	1.686	4.602	2.5	.349
10	5.064	1.671	4.278	40.2	.496	5.003	1.678	4.603	3.2	.348
11	5.117	1.680	4.270	43.3	.516	4.978	1.675	4.604	10.5	.356
12	5.131	1.678	4.266	45.1	.529	4.969	1.675	4.604	12.6	.342
Exhaust-nozzle setting, 210; bleed closed; $w\sqrt{\theta}/\delta$, 68.64 lb/sec										
Outer wall			4.290					4.513		
2	4.961	1.774	4.285	49.7	0.464	4.808	1.768	4.512	6.6	0.305
3	4.966	1.770	4.279	45.5	.468	4.891	1.766	4.511	6.1	.311
4	4.985	1.764	4.274	41.8	.476	4.866	1.757	4.511	5.9	.332
5	5.033	1.752	4.266	38.0	.493	4.879	1.750	4.509	4.4	.339
6	5.048	1.731	4.258	38.3	.501	4.890	1.735	4.509	1.7	.344
7	5.022	1.699	4.241	36.9	.499	4.921	1.696	4.506	.4	.357
8	5.005	1.679	4.226	34.9	.499	4.927	1.678	4.509	1.2	.359
9	5.003	1.673	4.217	38.4	.502	4.919	1.678	4.511	2.2	.355
10	5.006	1.671	4.207	40.1	.506	4.907	1.678	4.513	3.7	.349
11	5.030	1.678	4.201	43.0	.516	4.874	1.676	4.516	11.2	.334
12	5.062	1.683	4.196	45.5	.525	4.892	1.675	4.516	16.1	.341
Exhaust-nozzle setting, 180; bleed closed; $w\sqrt{\theta}/\delta$, 69.13 lb/sec										
Outer wall			4.218					4.440		
2	4.887	1.783	4.216	51.2	0.466	4.697	1.779	4.458	6.0	0.287
3	4.881	1.774	4.213	47.1	.468	4.741	1.768	4.457	5.4	.310
4	4.897	1.759	4.210	42.7	.471	4.786	1.739	4.455	5.0	.333
5	4.910	1.740	4.204	39.5	.478	4.805	1.727	4.454	3.4	.342
6	4.924	1.723	4.196	37.6	.485	4.821	1.717	4.452	1.8	.350
7	4.920	1.692	4.180	35.3	.490	4.853	1.691	4.451	-.5	.364
8	4.904	1.671	4.163	35.7	.491	4.848	1.671	4.452	.5	.361
9	4.901	1.666	4.152	37.3	.494	4.839	1.666	4.454	1.1	.357
10	4.902	1.669	4.140	40.4	.499	4.830	1.669	4.456	2.5	.352
11	4.914	1.675	4.152	42.0	.506	4.833	1.662	4.458	9.1	.353
12	4.931	1.681	4.127	45.2	.512	4.825	1.666	4.459	15.1	.348

Negative angles signify turning past axial direction.

[redacted]

Figure 1. - Test installation of five-stage axial-flow transonic compressor.

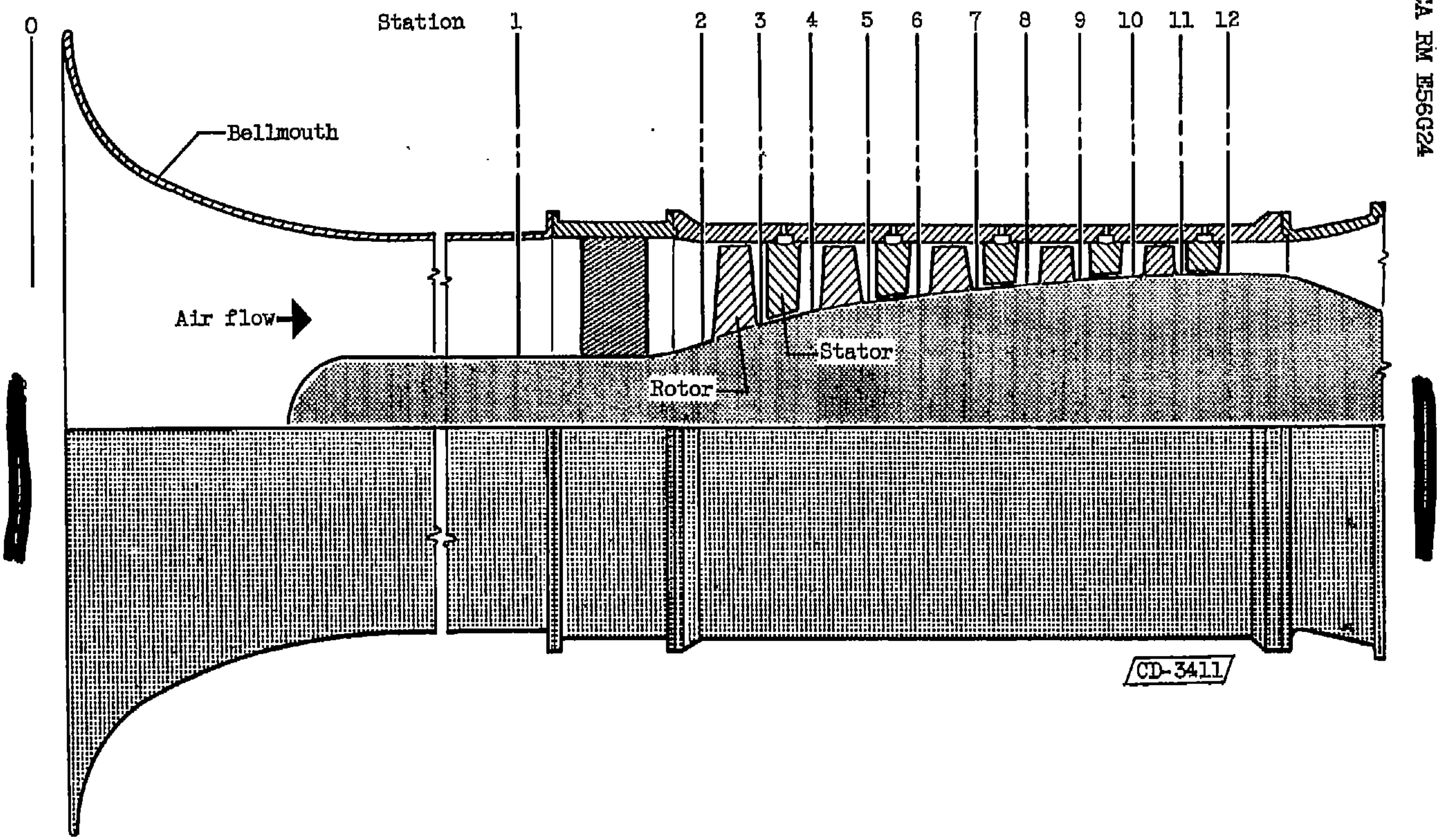

Figure 2. - Sketch of passage contour of five-stage axial-flow transonic compressor showing axial location of blade-row inlet and outlet stations.

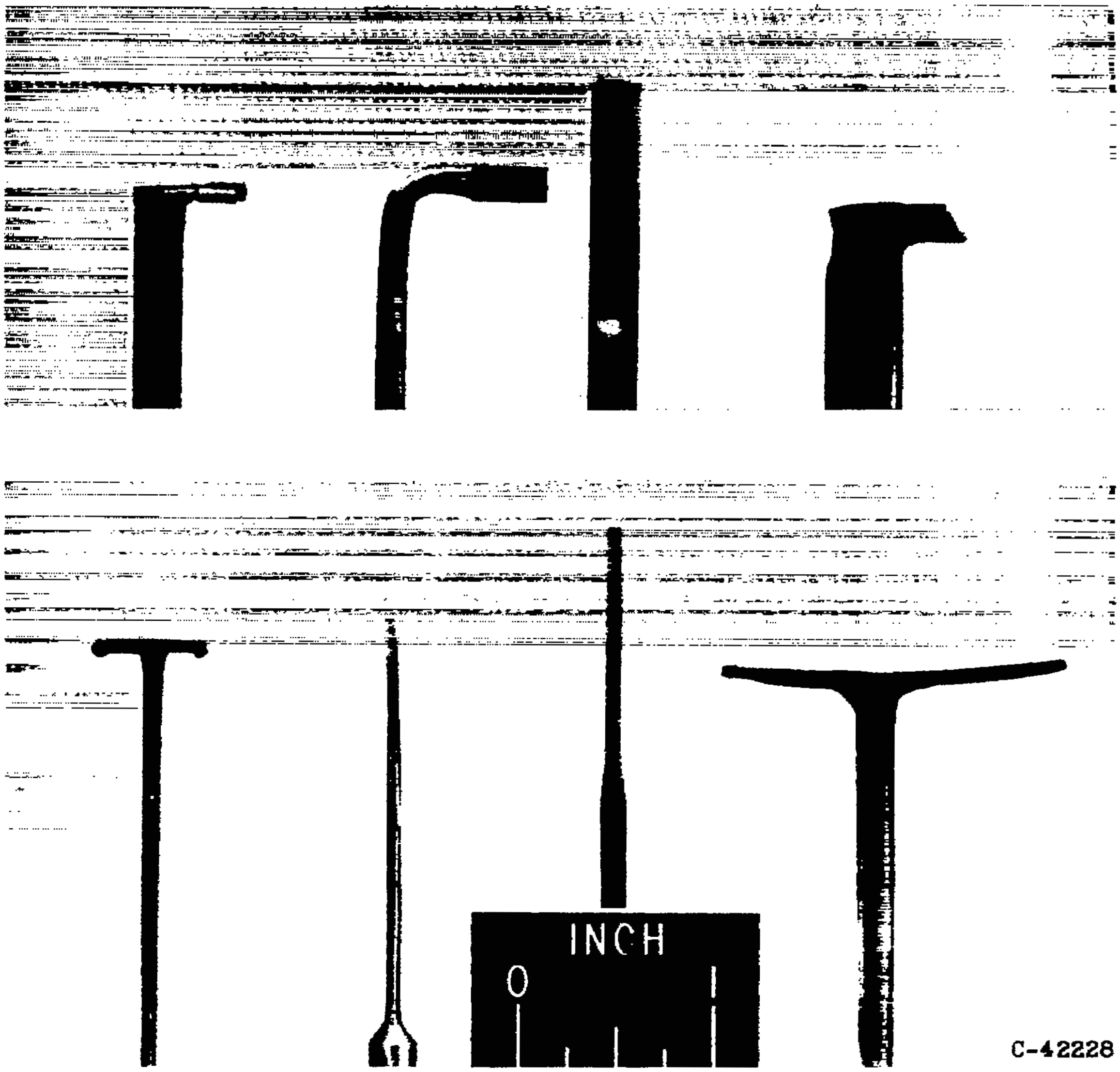

(a) Combination probe.

(b) Wedge static probe used at survey stations 3 to 12.

(c) Wedge static probe used at first-rotor inlet.

(d) Wake rake.

Figure 3. - Instrumentation used for radial surveys.

4154

CQ-5

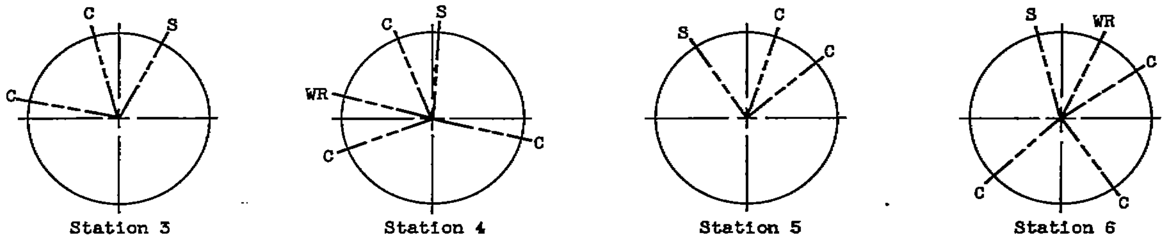

(a) First series.

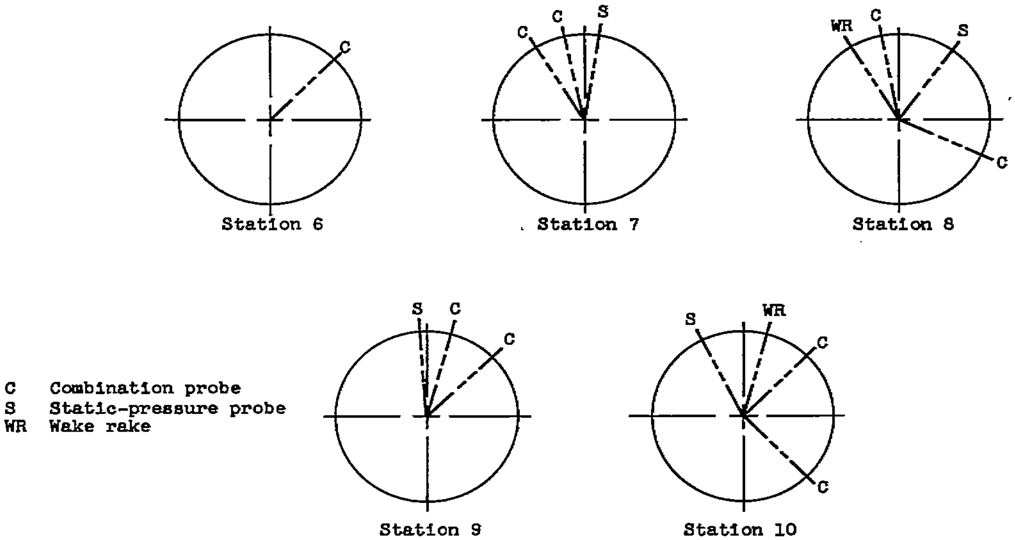

(b) Second series.

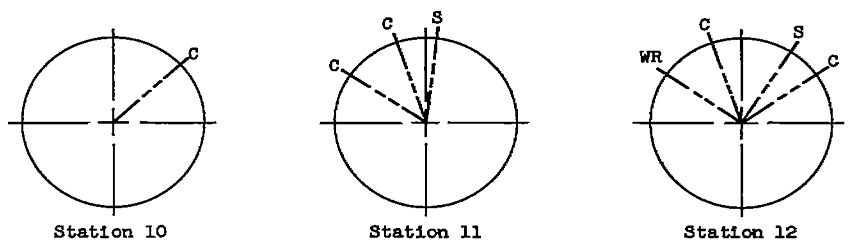

(c) Third series.

Figure 4. - Approximate circumferential location of probes viewed from upstream.

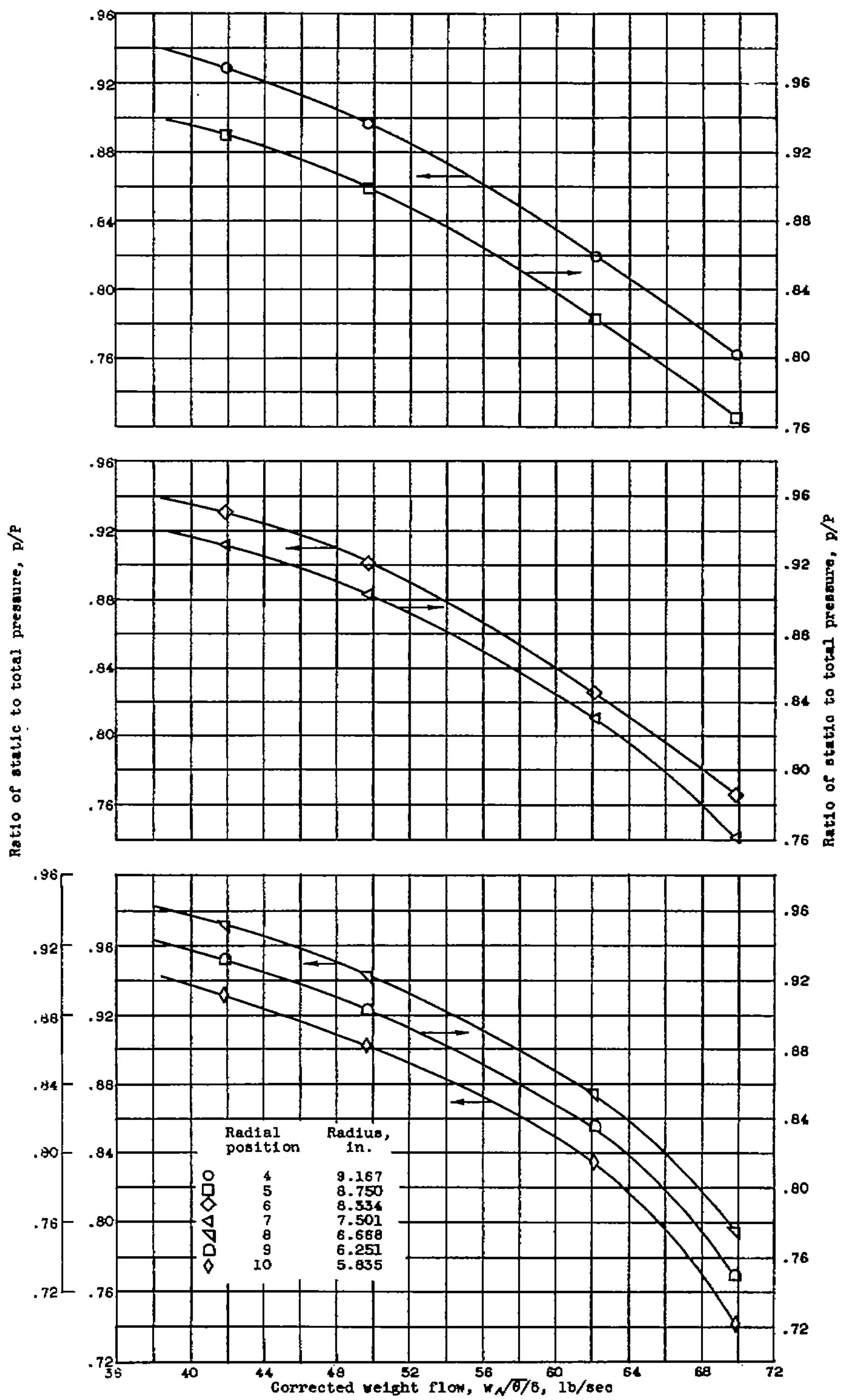

Figure 5. - Variation of static pressure with corrected weight flow for various radial positions at first-rotor inlet of five-stage transonic compressor.

[redacted]

4154

4154

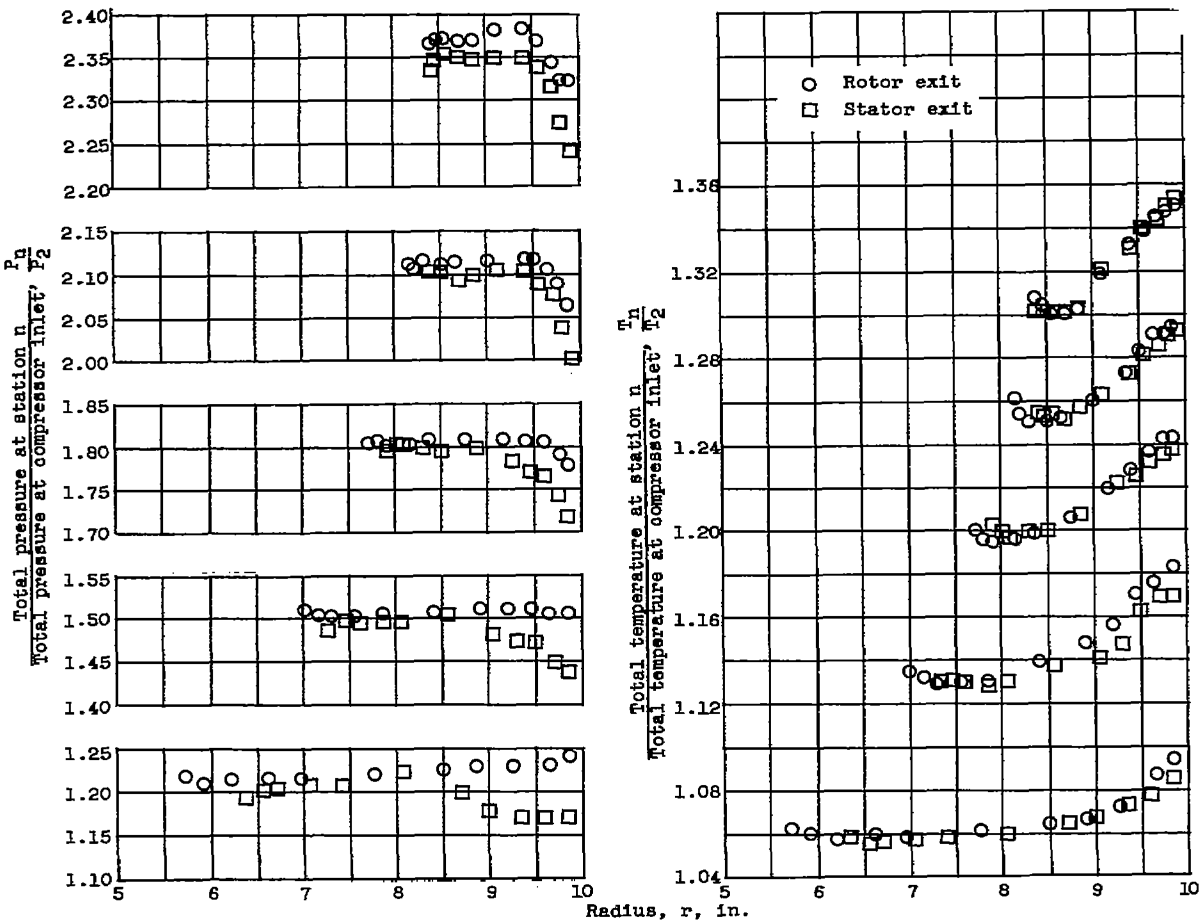

(a) Corrected speed, 70-percent design. Operation near peak efficiency.

Figure 6. - Radial variation of ratios of total pressure and total temperature at exit of each blade row of five-stage transonic compressor.

4154

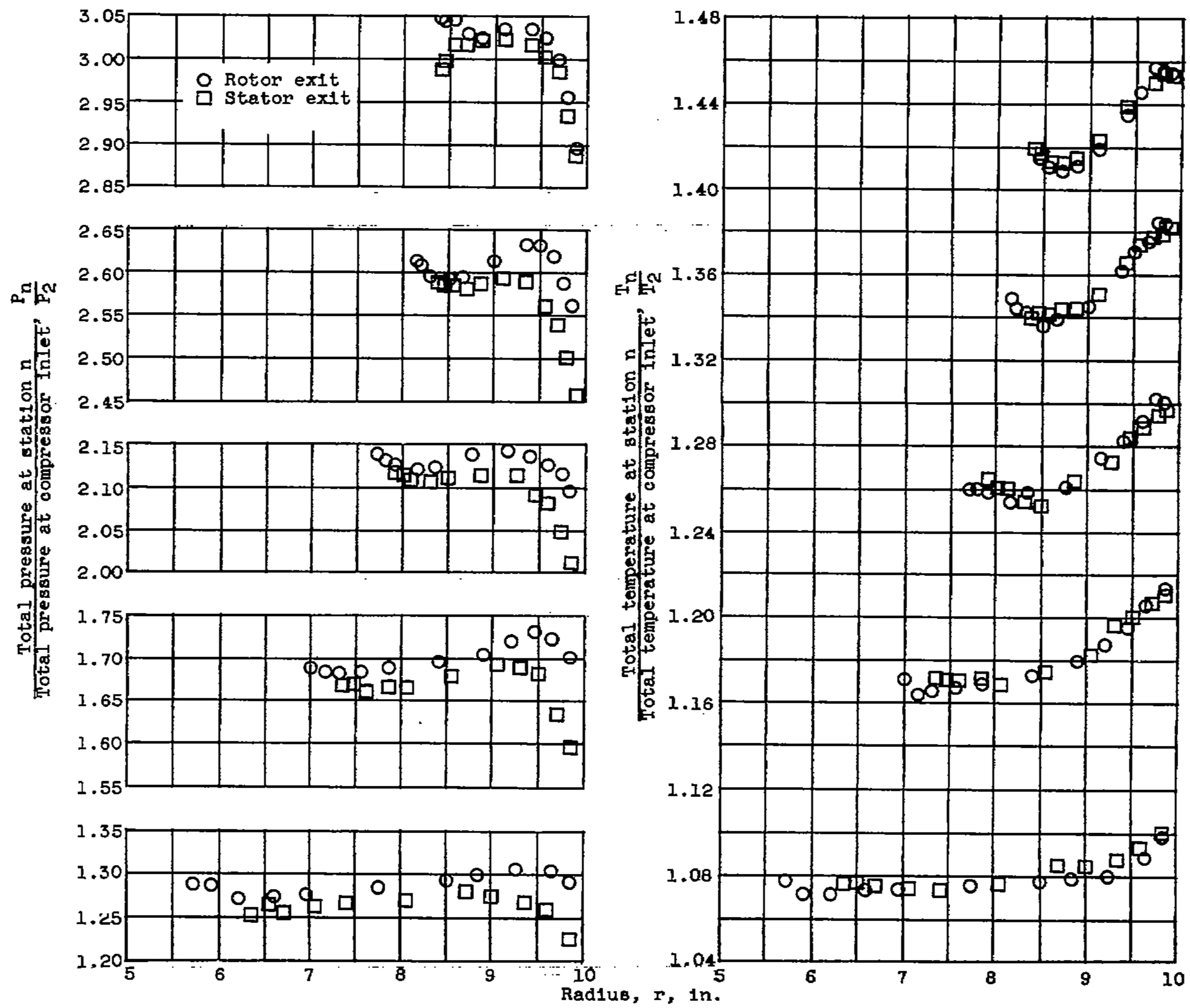

(b) Corrected speed, 80-percent design. Operation near peak efficiency.

Figure 6. - Continued. Radial variation of ratios of total pressure and total temperature at exit of each blade row of five-stage transonic compressor.

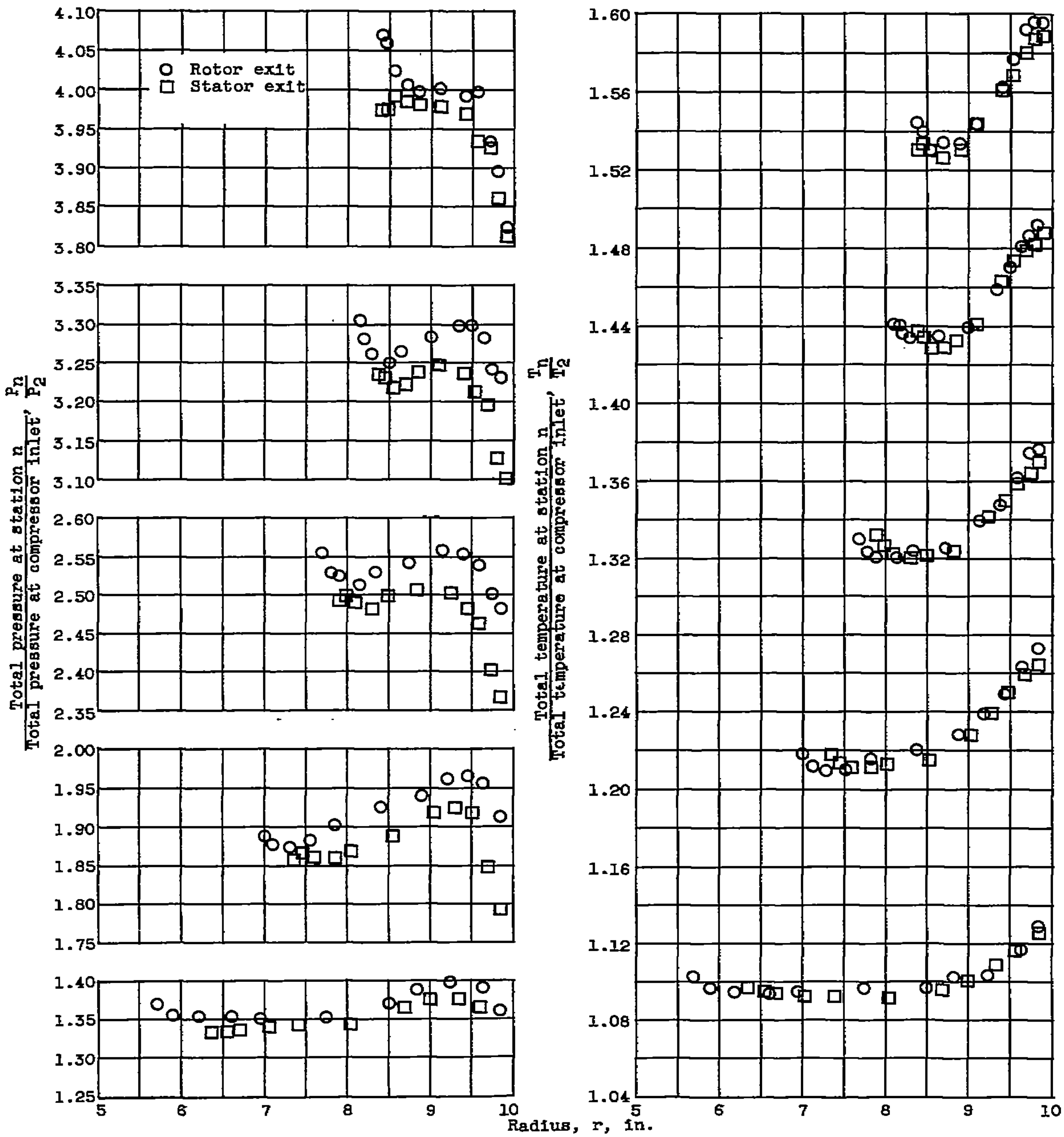

(c) Corrected speed, 90-percent design. Operation near peak efficiency.

Figure 6. - Continued. Radial variation of ratios of total pressure and total temperature at exit of each blade row of five-stage transonic compressor.

4154

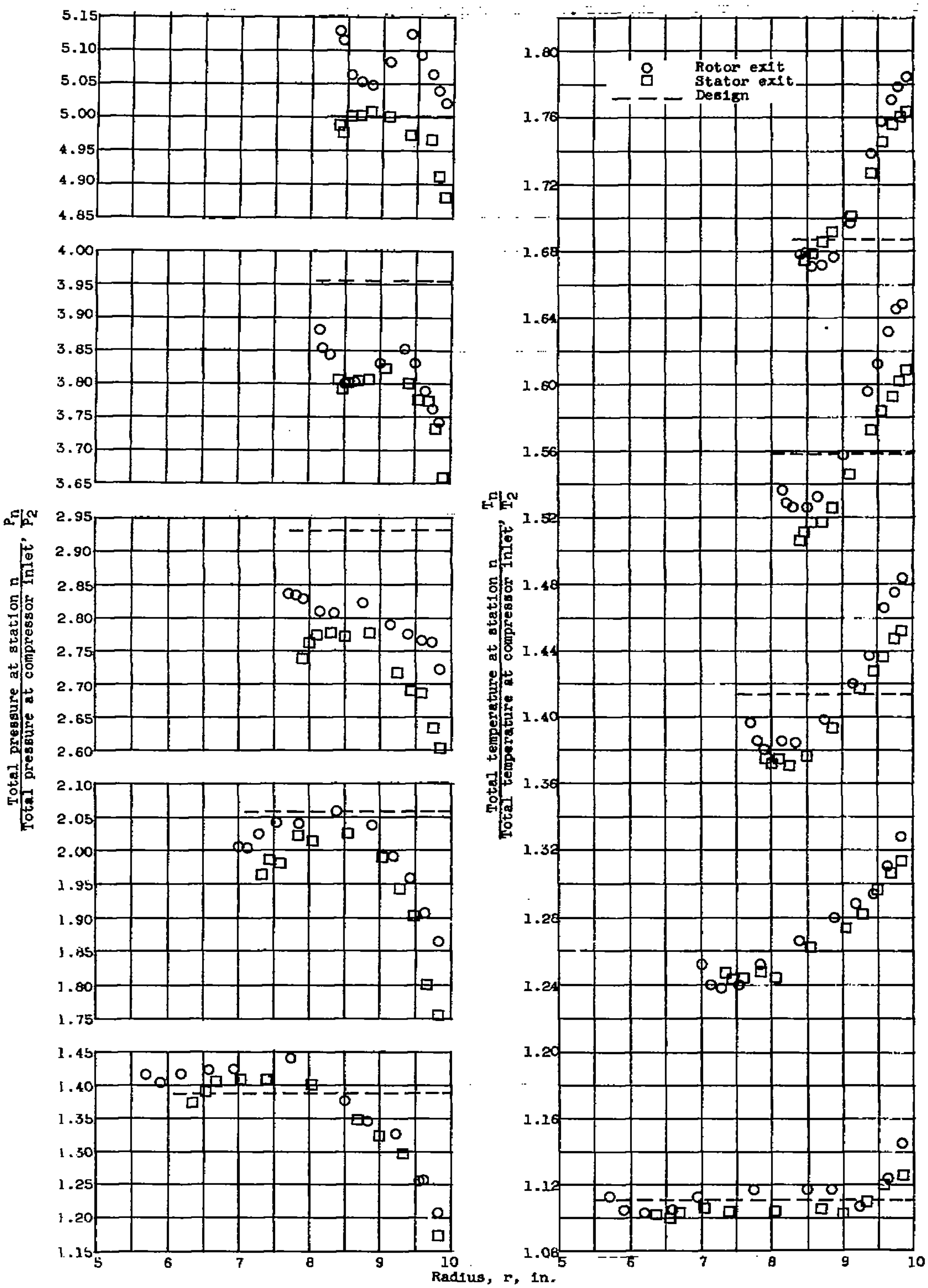

(d) Corrected speed, 100-percent design. Operation at design pressure ratio.

Figure 6. - Concluded. Radial variation of ratios of total pressure and total temperature at exit of each blade row of five-stage transonic compressor.

[redacted]

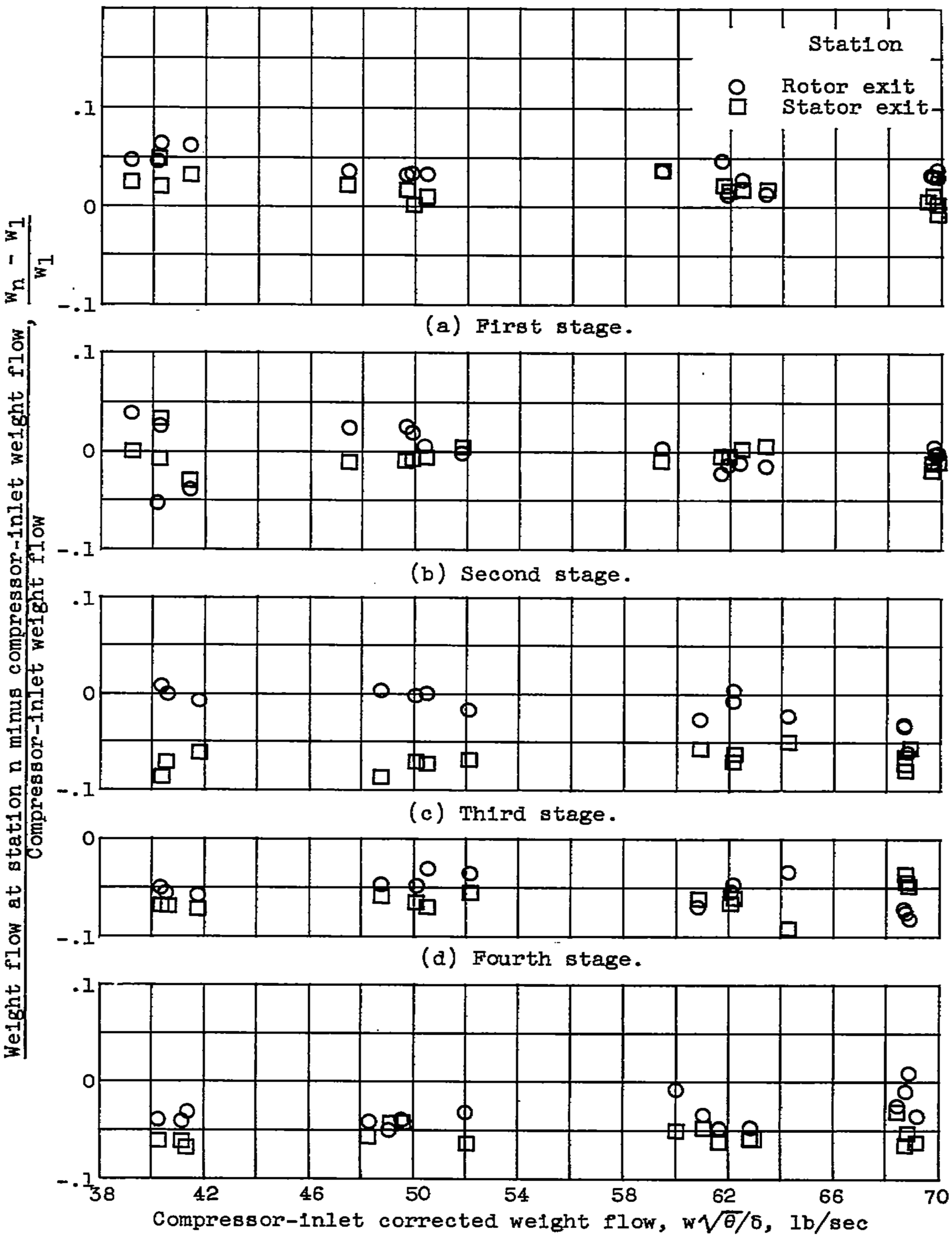

(e) Fifth stage.

Figure 7. - Comparisons of measured weight flows.

[redacted]

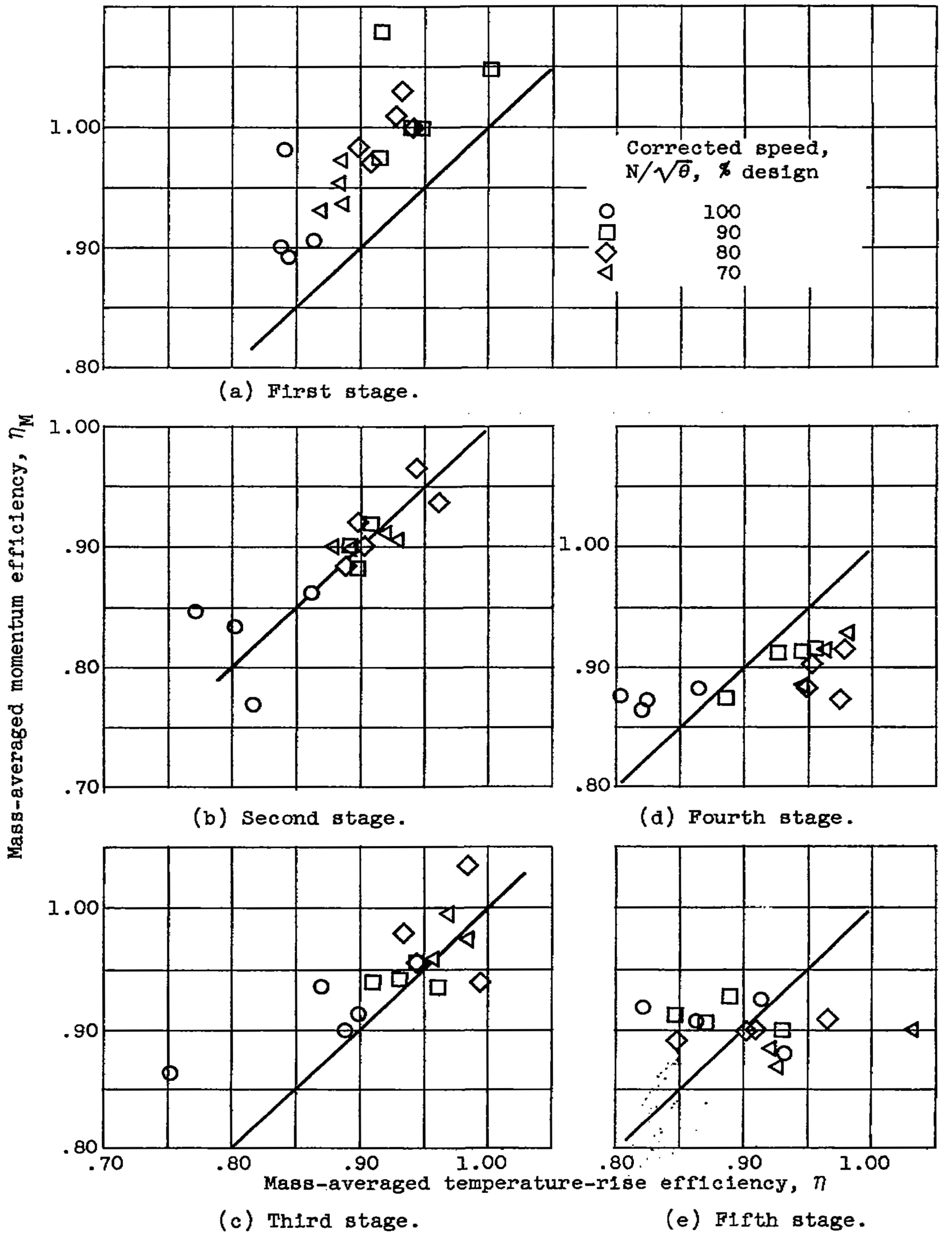

Figure 8. - Comparison of mass-averaged efficiencies.

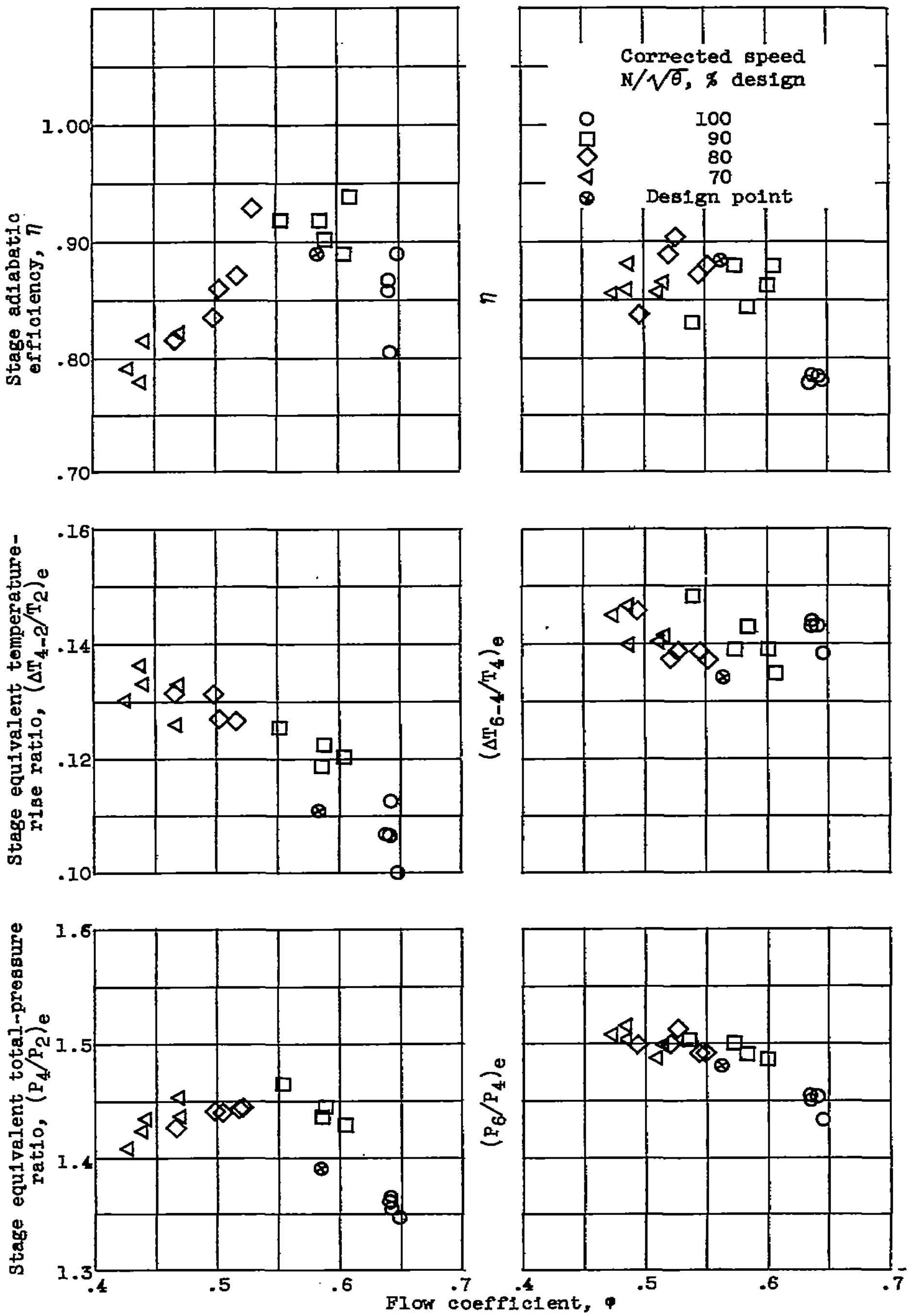

(a) First stage. (b) Second stage.

Figure 9. - Individual stage performance of five-stage transonic compressor.

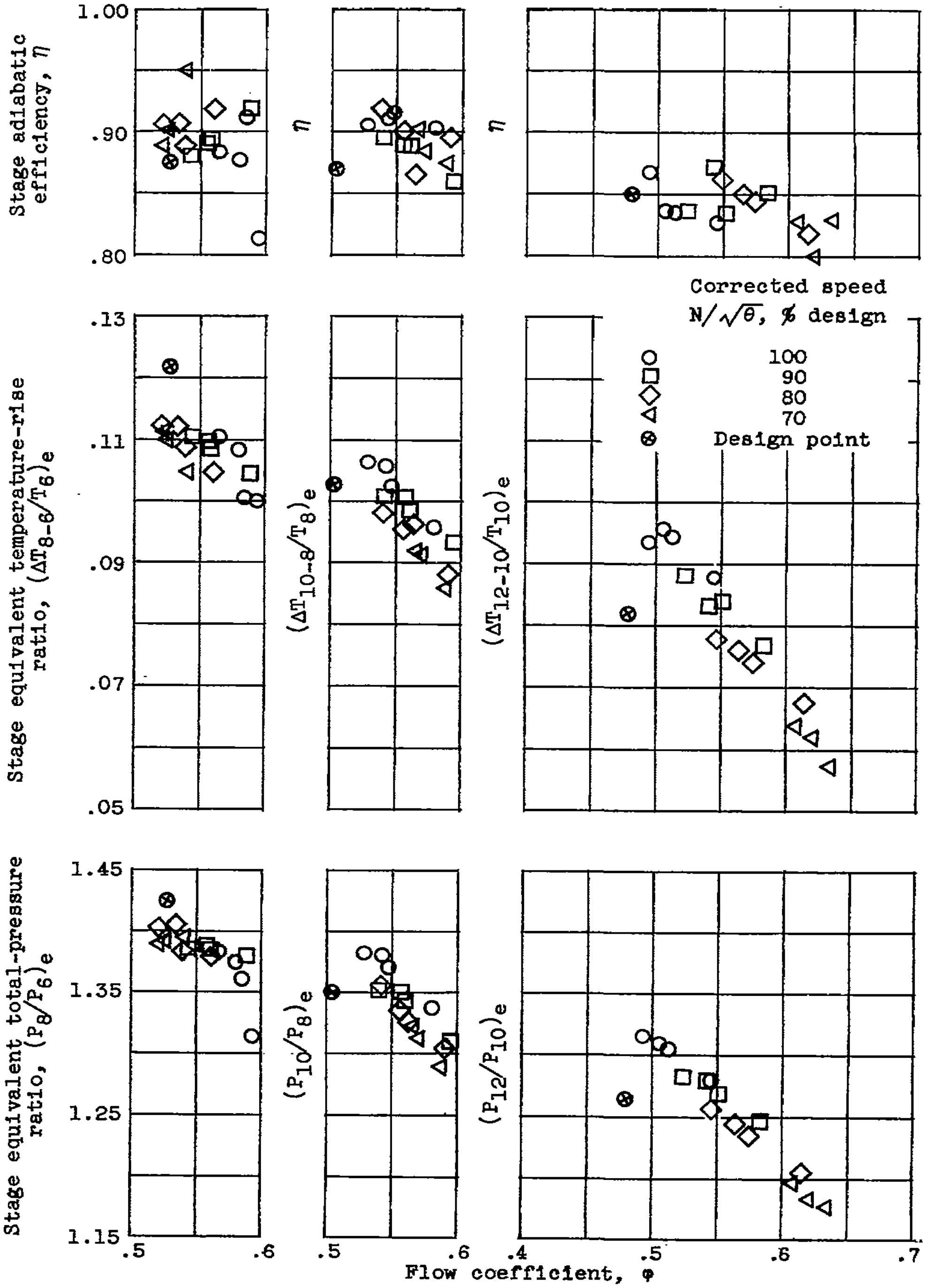

(c) Third stage.

(d) Fourth stage.

(e) Fifth stage.

Figure 9. - Concluded. Individual stage performance of five-stage transonic compressor.

[redacted]